EU contract number RII3-CT-2003-506395 CARE-Report-2007-015-SRF

SRF 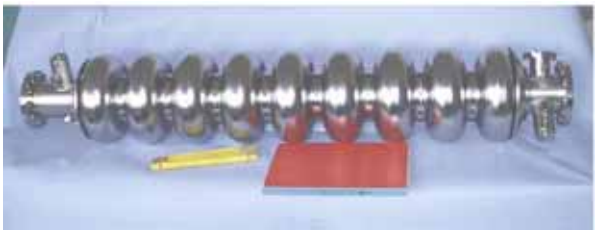

CARE JRA1 SRF Technology WP 8/ Task 8.4

Deliverable 8.4.8: Report on IN2P3 tuner activities

Task leader: **M. Fouaidy**

Full Characterization of Piezoelectric Actuators used for Superconducting RF Cavities Fast Active Tuning

M. Fouaidy[1], G. Martinet[1], N. Hammoudi[1], F. Chatelet[1],
1) IPNO, Université Paris-Sud 11, CNRS/IN2P3, Orsay, France

Abstract

Piezoelectric actuators are integrated as active element in Fast Cold Tuning Systems and used to compensate dynamically the frequency shift induced by high surface magnetic fields in Superconducting RF cavities. In the frame of the European CARE project, we designed and constructed three apparatus dedicated to the measurements of electromechanical (capacitance, loss factor, displacement), thermal (specific heat, interfacial thermal resistance) and dynamic properties (effect of a preloading force) of piezostacks for T in the range 2K-300K. Moreover, radiations hardness tests were also performed with fast neutrons beams at T=4.2K. The experimental data we obtained are analyzed and discussed.

Contents

Introduction

Due to their narrow bandwidth Δf_{BW}, Superconducting RF (SRF) cavities are very sensitive to small mechanical deformations which change the volume of the resonator. In particular, high electromagnetic fields (e.g., radiation pressure) induce mechanical deformations ranging from 0.1μ to 1μm of the thin (i.e., ~3mm-4mm) cavity wall, resulting in a frequency shift or Lorentz detuning $\Delta f_L \approx \Delta f_{BW}$ of these accelerating structures. More precisely, the radiation pressure P depends quadratically on the surface RF electric (E_S) and magnetic (H_S) fields according to the well-known relationship $P = \frac{1}{4} \cdot (\mu_0 H_S^2 - \varepsilon_0 E_S^2)$. For TESLA cavities, the radiation pressure P ~ kN/m^2 at an accelerating field E_{acc}=25MV/m. By using Slater formulae (e.g., $\frac{\Delta f_L}{f_O} = \frac{1}{4W} \cdot \iiint_{\Delta V} P \cdot dV$), where ΔV, f_0 and W are respectively the change of the resonator volume due to radiation pressure, the fundamental mode frequency and the electromagnetic energy stored in the resonator, the Lorentz detuning or frequency shift Δf_L is computed by numerical codes (e.g., coupled mechanical and electromagnetic computations). These simulations lead a quadratic dependence with the accelerating field namely $\Delta f_L = -K_L.E_{acc}^2$, where the Lorentz detuning factor K_L is a parameter depending on the cavity material, its shape and the boundary conditions. An additional RF power is then needed to operate the cavity at a given accelerating field E_{acc} if this detuning is not compensated. The ratio of the actual RF power P_{RF} to that needed in the ideal case P_{RF0} (e.g., with zero detuning) is given by the expression: $\frac{P_{RF}}{P_{RF0}} = 1 + \alpha . \left(\frac{\Delta f(t)}{\Delta f_{BW}} \right)^2$, where α is a constant depending on the matching conditions. The values of α are respectively 0.25 (with particles beam) and 1 (without the particles beam). Further, the measured detuning factor for TESLA cavities in pulsed mode operation (e.g., ILC machine: pulse duration= 1.3 ms, repetition rate= 5Hz, E_{acc}=33MV/m for a centre of mass energy E_{cm}=800GeV) is $K_L \cong 0.5\text{-}1$ Hz/(MV/m^2) leading to a maximum frequency shift Δf_L=1090 Hz at E_{acc}=33MV/m. For TESLA cavities, the bandwidth is Δf_{BW}=425 Hz. In such conditions, the RF power needed is increased by a factor 2.64 as compared to non detuned cavity. It is then mandatory to compensate this detuning in order to save power. Motorized Fast Active Cold Tuning System (FACTS) with integrated piezoelectric actuators will be used for adjusting and controlling the fundamental mode resonant frequency in SRF cavities of various projects and Test facilities (e.g., TESLA [1] Test Facility (TTF) [2], XFEL [3], ILC [4]). The motorized mechanical part of the FACTS, based on a steeping motor, is used for long range (i.e., 1.9mm or 820 kHz in terms of frequency tuning for TESLA nine cells cavity) and slow tuning purpose: it will compensate the frequency variations due to thermal effects (i.e., thermal contraction) during cool down of the resonator from T=300 K to the operating temperature T=2 K. On the other hand, the piezoelectric actuators will be used to compensate at high speed (i.e., 10^4 μm/s) the detuning Δf_L due to Lorentz forces of the accelerating cavity (i.e., tuning range: 3μm for Δf_L=1kHz). Such FACTS, using commercial piezoelectric actuators as active elements for deforming the resonator, was successfully applied to dynamic compensation of Lorentz detuning TESLA cavities [5] as illustrated in Fig. 1.

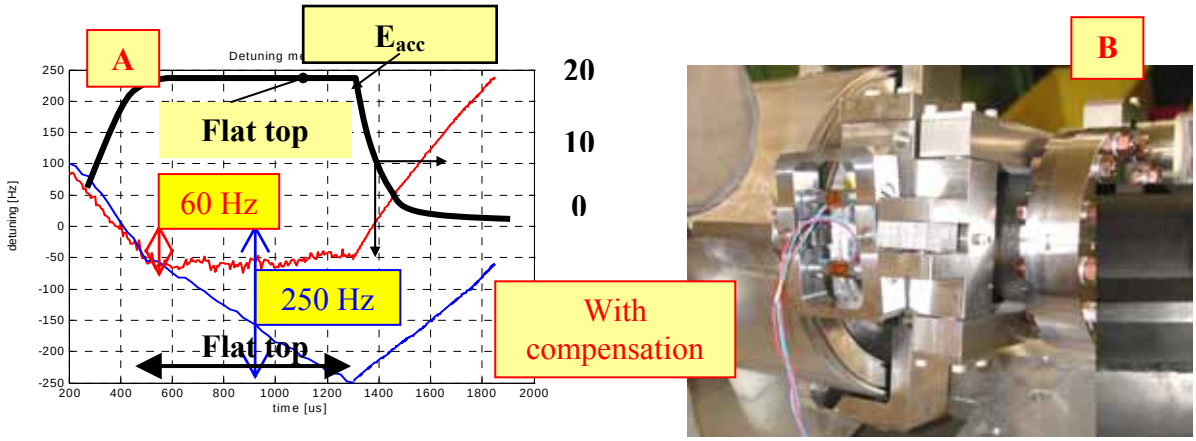

Figure 1: Compensation of detuning by a piezoelectric actuator in a TESLA cavity for a flat top gradient E_{acc}=20MV/m (black curve) (A). Actuators attached to the tuning system (B).

The data of Fig. 1 show that the value of the Lorentz detuning is reduced from Δf_L~-250Hz without compensation down to Δf_L~-60Hz with dynamic compensation. Further, during the flat top of E_{acc} (e.g., beam on), the variations of Lorentz detuning are δf_L ~-10 Hz (with compensation) and δf_L ~-200Hz (without compensation).
Due to the lack of experimental data (e.g., electromechanical, dynamic and thermal properties) for the operating conditions of the piezoelectric actuators in the cryomodule and accelerator environment (vacuum: 10^{-5} mbar, cryogenic temperatures, ionizing radiation), an experimental program aiming at full characterization of piezoelectric actuators at low temperature (i.e., 1.8 K-300K) was launched in the frame of the CARE project WP8 concerning the development of tuners. Moreover, the piezoelectric actuators may be located in the radiation environment induced by field emitted electrons or dark current (γ rays) and/or occasional beam losses during machine operation (i.e., γ rays and fast neutrons). In order to provide for a reliable operation of the machine, these components (~24.000 units) should function satisfactorily for long periods (e.g., ideally case: machine life duration) even when subjected to intense radiation (e.g., neutrons fluence up to 10^{12} n/cm^2 [6]).
In this report, we will describe the experimental facilities developed at IPN Orsay for studying the electromechanical, dynamic and thermal properties of prototype piezoelectric actuators and will analyze the experimental results, we obtained. This study includes also, the investigation of the effect of fast neutrons radiation on actuators properties, lifetime and performance.

Characterization at low temperature: experimental set up and test procedure

The piezostacks tested

Although, their internal structure and the fabrication process are different, all the industrial low voltage actuators we tested are of multilayer type piezostacks (Fig. 1) and are based on PZT active material (PZT: Lead Zirconate Titanate). These piezostacks were supplied by

three different companies: Piezosystem JENA, PI and NOLIAC. The main characteristics of these actuators, which behave basically as capacitors, are illustrated in Table 1.

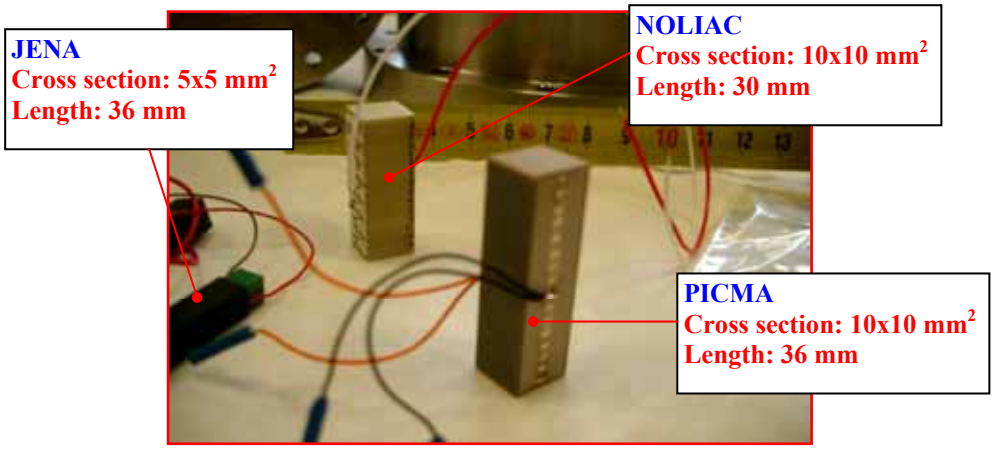

Figure 1: Piezoelectric actuator (material: PZT).

Table 1: Main characteristics of the piezostacks tested.

Supplier / Parameter (unit)	NOLIAC	Physical Instruments	Piezosystem JENA
Type	PZT pz27	PZT 25	PZT
Length (mm)	30	35	42
Section (mm^2)	10x10	10x10	5x5
Young modulus (GPa)	45	37	50
Displacement at T~300K (µm)	42	35	40
Frequency (kHz)	66	40	?
Stiffness (N/µm)	150	105	25
Blocking Force (kN)	6.3	3.6	1
Capacitance @ 300K (µF)	5.7	12.4	3.4
Maximum voltage V_{max} (V)	200	120	150

Test cell description

The apparatus dedicated to the tests of the actuators must fulfil the following main requirements:

-calibration and full characterization of piezoelectric actuator under vacuum and at controlled low temperature T (1.8 K –300 K),
- avoid shear forces and torsion forces to the actuator,
- allowing mechanical pre-loading to the actuator for dynamic operation.

Two test-cells were used for this experiment [7]. A schematic diagram and a photograph of the first test-cell developed are shown in Fig. 2 and Fig. 3. The actuator is clamped between two stainless steel cylindrical supports (diameter: 20 mm, thickness: 10 mm) then inserted into a special holder. This holder includes three stainless steel main flanges (diameter: 82 mm,

thickness: 15 mm), Belleville rings acting as springs and supporting rods (diameter: 12mm). The actuator supports are attached to the main flanges, in which conically shaped groves are machined, via small stainless steel balls (diameter: 6mm) in order to avoid shear and torsion forces, which would damage the piezostacks. Moreover, in order to increase the tensile strength of the piezostacks during dynamic operation, a bronze screw acting axially on the lower flange allows the adjustment of the actuator preload (up to ~10% of the maximum preload F_{max}=1 kN). The whole assembly is enclosed in a vacuum chamber. Notice that the bottom extremities of the three supporting rods are rigidly fixed to the chamber. Furthermore, three calibrated thermometers (platinum resistor, Allen-Bradley carbon resistors and cernox^{TM} resistors) and a manganin heater wrapped around a small stainless steel piece attached to the actuator are used to control and measure the piezostacks temperature.

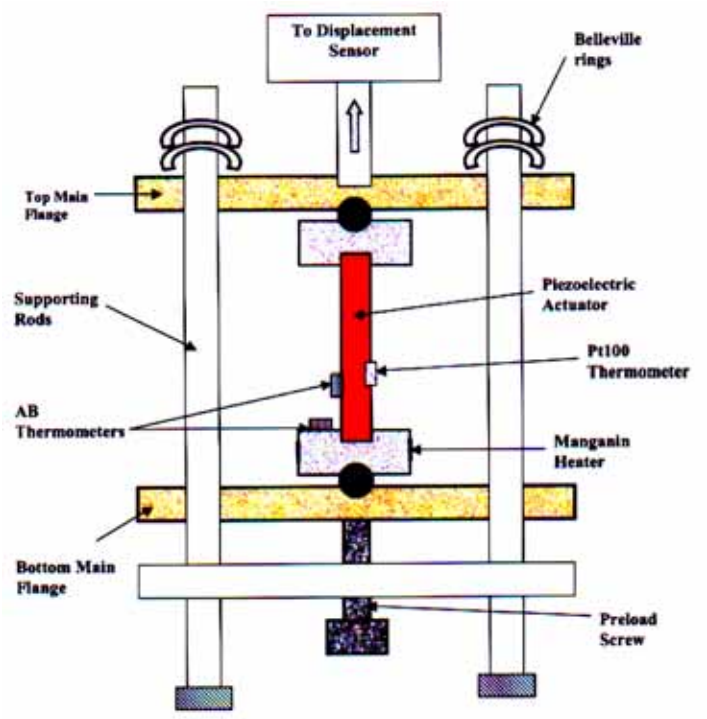

Figure 2: Diagram of the Test-Cell.

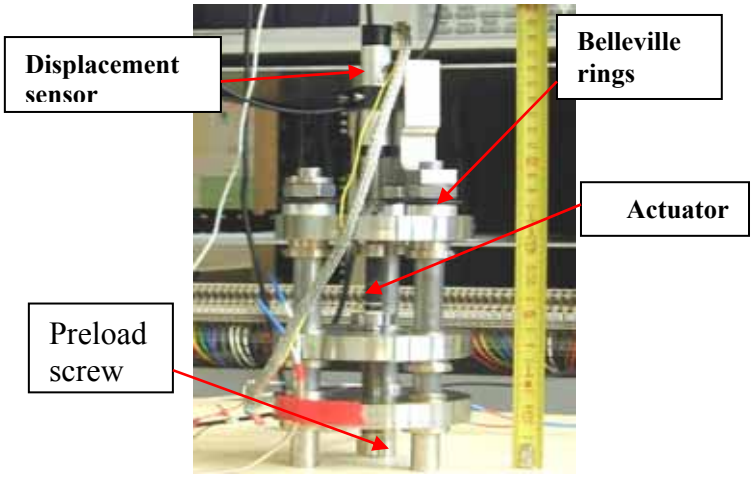

Figure 3: Test apparatus prior to installation into vacuum chamber (First test-cell).

Finally, a mechanical assembly including stainless steel rod (diameter: 14 mm) and bellows allows the transmission of the motion induced by the actuator in operation to a resistive displacement sensor operating at room temperature and located on the upper flange of the cryostat insert. The first test-cell has a main drawback: it takes a too long time to cool down. This is due to the large thermal capacity of stainless steel part of the system (supporting rods and main flanges). So we developed a second test-cell (Fig. 4), which consists mainly in a cylindrical vacuum chamber with a removable thin end plate. The actuator is sandwiched between the lower rigid flange (thickness: 32.5mm) and the upper thin stainless steel sheet (thickness: 0.2mm). The system includes stainless steel ball with special fixture to avoid shear and torsion forces on the piezostacks, which is equipped with a heater and calibrated temperature sensors. Briefly, the operating principle is the following: when a voltage is applied to the piezoactuator, it expands leading to a deformation of the upper thin sheet; the resulting motion is transmitted to the displacement sensor at room temperature via a stainless steel rod.

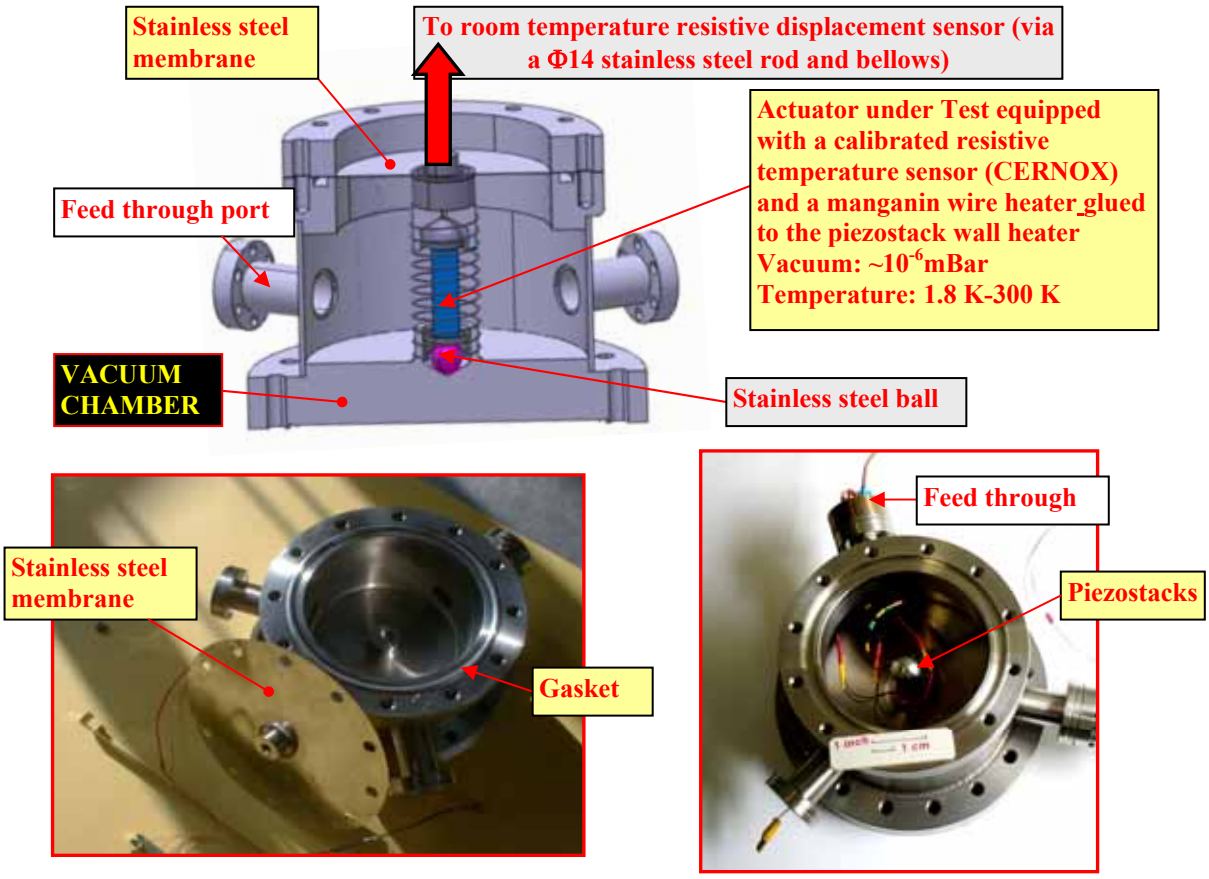

Figure 4: 3D drawing and photographs of the second test-cell.

Experimental procedure

Prior to the tests at low temperature, the displacement sensor is calibrated at T≅ 300 K using the piezoelectric actuator as a reference and the supplier calibration data (i.e., displacement versus actuator voltage). The low temperature tests were performed for T in the range 1.8K-

300K, using either Liquid Nitrogen (LN_2) or Liquid Helium (Lhe) as cryogenic liquid. The test-cell is evacuated down to 10^{-5} mbar then cooled down to 77 K (normal boiling point of nitrogen) or 4.2 K (normal boiling point of helium). A thermal switch is used to improve the cooling rate in the case of the first test-cell: the chamber was pressurized up to ~200 mbar with high purity gaseous helium (99.995%). Notice that due the strong temperature dependence of the specific heat C of materials (e.g., $C= aT + bT^3$), the thermal switch is only used for temperatures higher than 80 K. Once the piezostacks actuator is at LN_2 or Lhe normal boiling point temperature, the test-cell is evacuated again down to ~10^{-5} mbar. The actuator temperature T is then regulated at the desired value and measurements are performed. In the course of the experiments, several parameters were investigated: a) displacement versus voltage characteristics at different temperatures T, b) actuator capacitance Cp vs. T, c) dielectric properties (dielectric constant: ε_r, and loss factor: tg(δ) as function of T using a LCR meter, d) heating ΔT due to dielectric losses as function of the frequency f and amplitude V of the sinusoidal signal applied to the piezostacks at different temperatures.

Tests results with Piezosystem JENA actuators

Several low voltage piezostacks of different productions series fabricated by Piezosystem JENA Company were tested. Most of these actuators showed electrical breakdown during the tests at cryogenic temperatures. As illustration, we present in Figure 5, the response (sensor signal) of the displacement sensor to voltage applied to the actuator #8114 at T=295 K: the sensing current in the displacement sensor is 40 µA. Notice that each stage in the curve of Fig. 5 corresponds to the indicated voltage applied to the actuator (label).

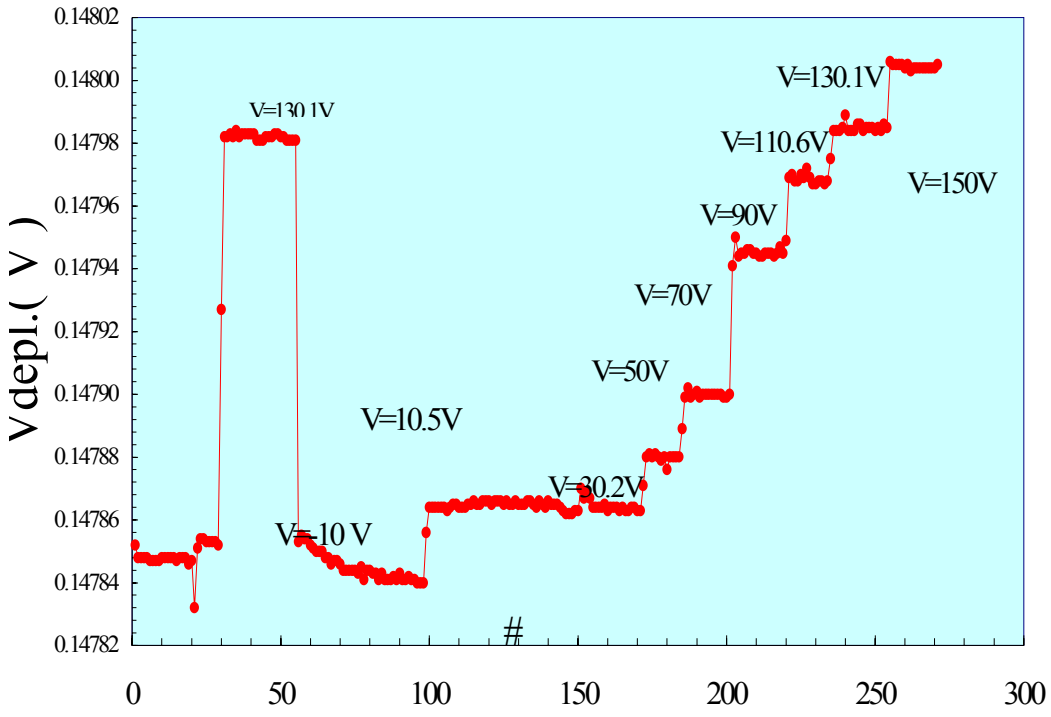

Figure 5: Displacement sensor signal versus applied increasing voltage: Actuator #8114.

Reproducibility tests at Room Temperature (RT)

Reproducibility tests were performed on the same actuator at T=295 K, while increasing the applied voltage Vpiezo from –10V to 150V (full range). The corresponding data are shown in Fig. 6.

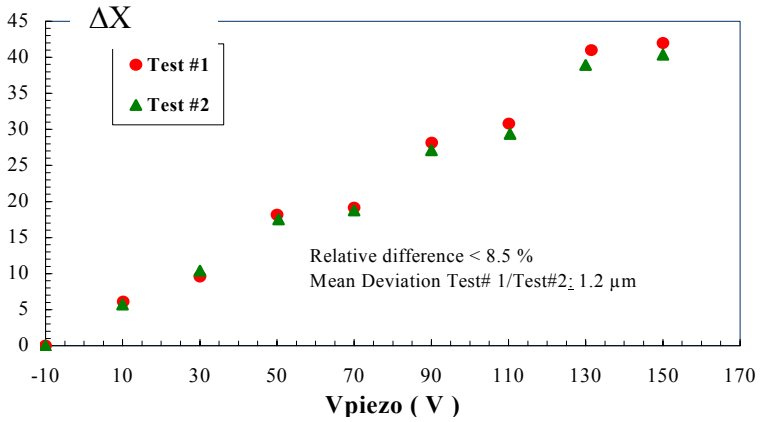

Figure 6: Reproducibility tests at T=295 K-Actuator #8114.

The full range displacement at T=295 K is 42.1 µm. The observed differences between the two runs are attributed to mechanical hysteresis in the system and measurement errors: the mean standard deviation between the two runs is 1.2µm and the relative difference is less than 8.5%.

Calibration: displacement versus actuator voltage at different temperatures

a) Actuator # 8114

The displacements versus actuator voltage characteristics were measured at different temperatures T between 77 K and 300 K. The response of the actuator #8114 at T=77 K is presented in Fig. 7. As expected, the displacement at a given actuator voltage decreases strongly with T.

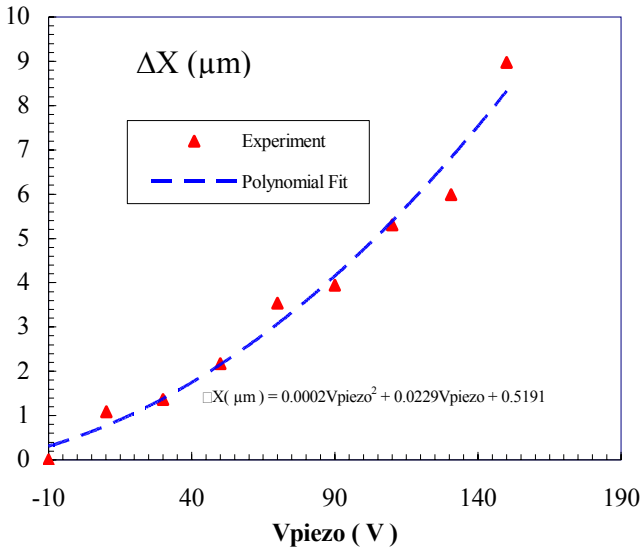

Figure 7: Displacement versus actuator voltage at T=77 K (actuator#8114).

The full range displacement is decreased by a factor of ~ 4.7 when T decreases from 300K down to 77K and this result is in the range of data reported previously by other authors [8-9]. Moreover, the variations of the full range displacement or maximum actuator expansion ΔX with temperature are shown in Fig. 8 for the same actuator # 8114. The slope of the curve ΔX vs. T curve decreases strongly with temperature. This non linear behaviour is mainly due to the strong dependence of the actuator capacitance on temperature as we will show later in this paper. Unfortunately this actuator was damaged (e.g., electromechanical breakdown) at the end of these first tests.

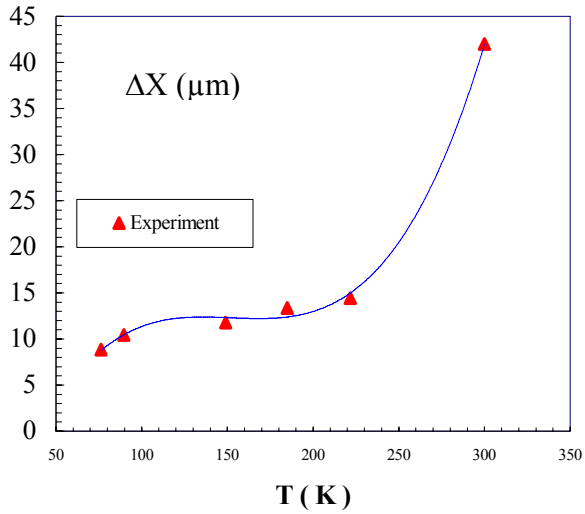

Figure 8: Variations of the full range (V_{max}=150 V) displacement with temperature (piezo #8114).

b) Actuator # 9221

This actuator is from a second series. As we have no data for temperature lower than 77 K, we performed the first experiment in liquid helium. These tests allow us to measure the full range displacement ΔX for temperatures between 1.8 K and 52 K as shown in Fig. 9. Note that at Room Temperature (R.T), the manufacturer calibration data gives ΔX=42.6 µm.

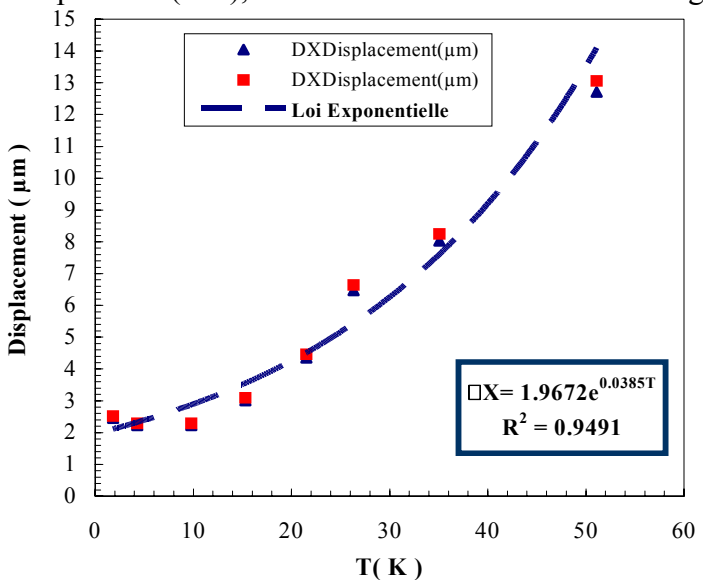

Figure 9: Full range (V_{max}=150 V) displacement at low temperature for actuator #9221.

The two sets of experimental data of Fig. 9 correspond to 2 calibrations at R.T showing a relative variation less than 2.7%. Moreover, these results show that the maximum actuator expansion decreases exponentially with temperature thus confirming previous observations reported by other authors [8-9]. Finally, for T≤10 K the maximum displacement is nearly constant: the observed variations are in the range of experimental errors.

Dielectric properties

In the course of the experiments, we measured by a LCR meter, the dielectric properties (e.g., capacitance, complex impedance, loss factor) of the actuators at three frequencies (100Hz, 120 Hz and 1kHz). However, only data at f=100 Hz will be presented in this report. For the actuators #8114 and #9220, the measurements were performed for T ranging from R.T down to 90 K while for the actuator #9221 the measurements were performed at R.T and in the temperature range 1.8 K-52 K.

a) Capacitance and dielectric constant versus T

The variations of the capacitance of the piezostacks with temperature are presented in Fig. 10 for the three actuators tested.

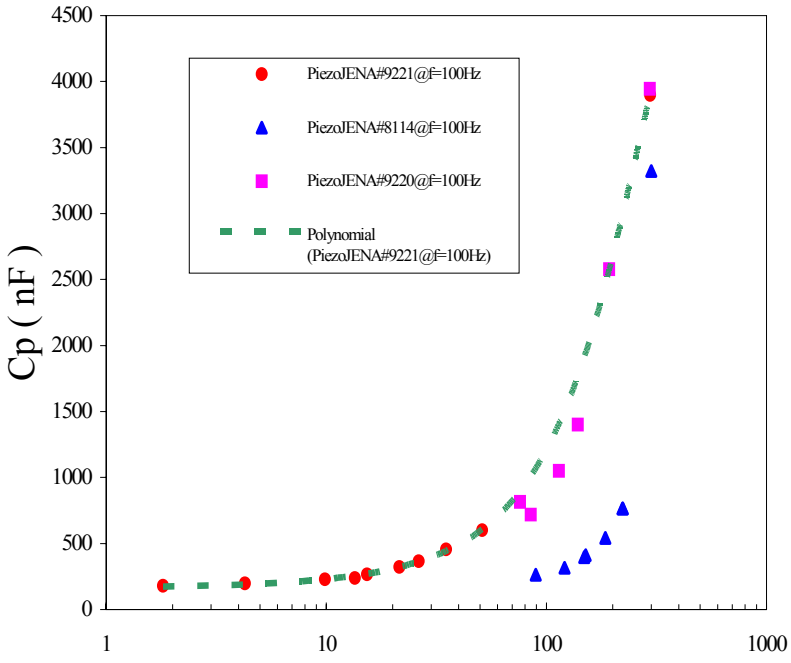

Figure 10: Capacitance versus T for three actuators.

The capacitance decreases dramatically (e.g., factor ~22) from ~3900 nF at R.T to ~180 nF at 1.8 K (actuator #9221). The piezostacks of the same production series (#9220 and #9221) have nearly the same temperature dependence and their values are close together. On the other hand, the actuator #8114 of a second production series has a quite different behaviour: its capacitance depends more strongly on temperature, resulting in a much lower full range displacement. Consequently, if piezostacks of different production series from Piezosystem JENA are used, it is recommended to perform careful individual calibration (i.e., ΔX vs. T).

Furthermore, at low temperature (i.e., T≤52 K), the full range displacement is proportional to the actuator capacitance as shown in Figure 11. It decreases down to its value at T ~ 10 K and stay nearly constant to within experimental errors for T<10 K.

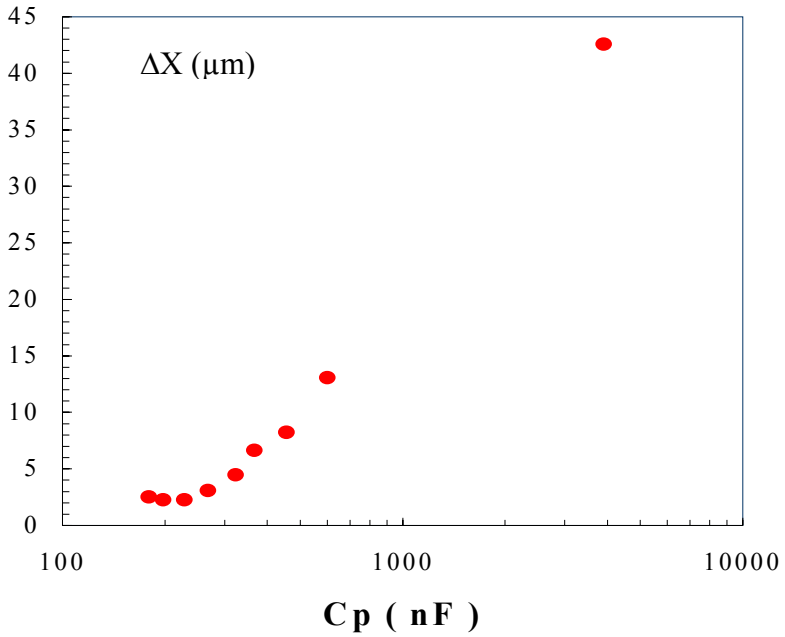

Figure 11: Full range displacement versus capacitance (actuator #9221).

The results of Figure 11 are very important: it might give another mean and a more simple way to calibrate actuators, but more statistics are needed (i.e., calibration and Cp vs. T measurements) to confirm this behaviour (i.e., $\Delta X \propto Cp$). It should be emphasized that capacitance measurements are simpler and less time consuming, as compared to a true calibration (i.e., displacement versus voltage applied to actuator at different temperatures).
The actuator from Piezosystem JENA consists of n=350 thin layers (thickness e=100 μm) of electro-active ceramic material (PZT) electrically connected in parallel. The capacitance is thus simply given by the well-known expression:

$$C_p = \frac{n.\varepsilon_0.\varepsilon_r.A}{e} \qquad (1)$$

With:
ε_0: permittivity of vacuum,
ε_r: dielectric constant of the material,
$A=25mm^2$: electrode surface area.

Using the above expression and experimental data namely Cp vs. T, we calculated the variations of the dielectric constant ε_r as function of temperature. Obviously, if the thermal contractions are neglected (e.g., layer thickness is constant), the dielectric constant is proportional to the capacitance (e.g., $\varepsilon_r \propto Cp$). As expected, the corresponding data shown in Fig. 12 are very similar to Cp vs. T curves.

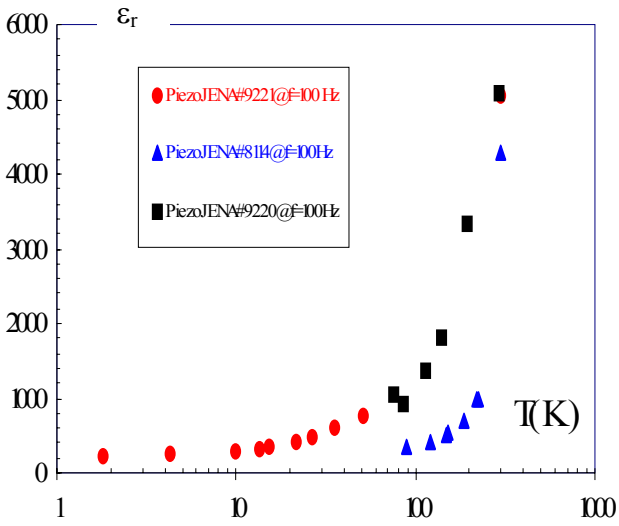

Figure 12: Dielectric constant vs. T for three actuators.

b) Dielectric losses

The measured loss factors (i.e., tg(δ)) for the three actuator tested are plotted in Fig. 13. In contrast to the other parameters such as ΔX, Cp and ε_r, the loss factor did not show a monotonous decrease with the temperature: more precisely, from its R.T value tg(δ) increases as T is decreased then reaches a maximum around T≅50 K, afterwards it decreases as T is lowered down to 1.8 K.

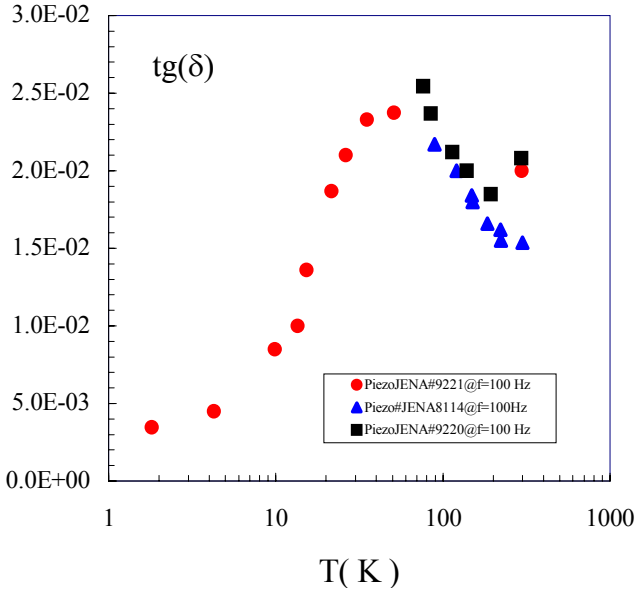

Figure 13: Variations of loss tangent with temperature.

More investigation is needed to understand the loss factor versus temperature behaviour of this material and in particular the existence of a peak in tg(δ) vs. T curve . Notice that this parameter reaches its minimum value (e.g., tg(δ) ≅ 3.510^{-3} at T=1.8 K for f= 100 Hz) in

temperature region of interest for SRF cavities (e.g., T≤ 4.5K). From the above results (e.g., calibration, Cp vs. T and tg(δ) vs. T), we calculated the total dissipated power or dielectric losses as function of temperature (Fig. 14) for a sinusoidal motion of 1µm amplitude of the actuator operating at a frequency f=100 Hz.

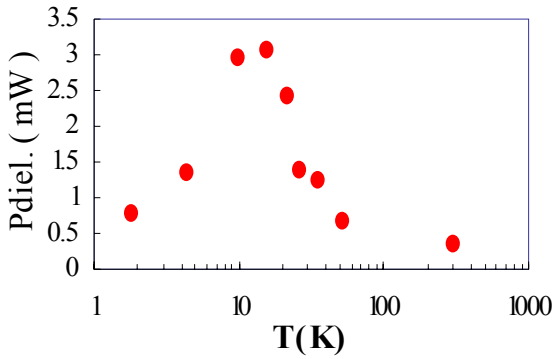

Figure 14: Total dielectric losses for a sinusoidal motion of 1µm amplitude at 100 Hz.

We recall that for TESLA cavities, a longitudinal deformation of 3µm corresponds to a Lorentz detuning compensation of ~1kHz. The results of Fig. 14 clearly show that dielectric losses of these actuators (piezostacks volume: 900mm^3), operating in such stringent conditions (e.g., full compensation at high repetition rate) are low (≤7mW) as far as the cryogenic budget is concerned. Furthermore, when the actuator is subjected to a sinusoidal voltage of amplitude V and frequency f, the total dielectric losses P_{diel} are given by the well-known relation ship:

$$P_{diel}=\pi.f.Cp.V^2.\sin(\delta) \qquad (2)$$

We measured the heating due to dielectric losses at different temperatures in two different conditions: 1) at a given fixed voltage amplitude V (sinusoidal signal) and variable frequency f, 2) at a given frequency and variable voltage amplitude. A typical result illustrating the first case is presented in Fig.15.

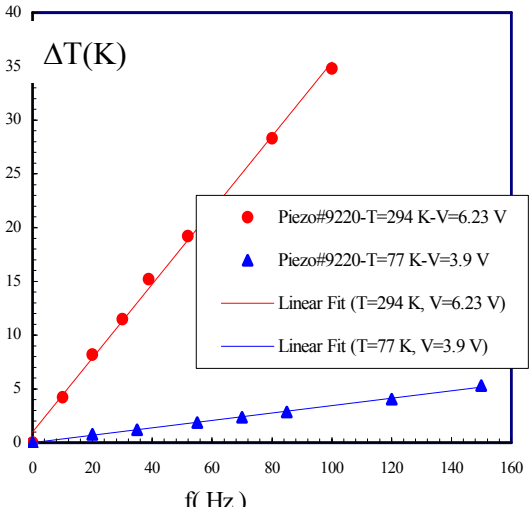

Figure 15: Heating due to dielectric losses: effect of signal frequency.

The measured heatings of Fig.15 clearly show a linear dependence on frequency at the two test temperatures namely T=294 K and T=77 K. This linear dependence is in good agreement with the above formulae (e.g., $\Delta T \propto P_{diel} \propto f$). Furthermore, for the two modulation voltages used in these tests and f=100 Hz, the ratio of the measured heating respectively at T=295K and T= 77K is ≅ 10.3 and this value is very close to the ratio (≅ 10.1) of the dielectric losses at these two temperatures, as given by the above formulae. This agreement is obviously observed at the other frequencies because the results show the linear dependence of P_{diel} with respect to f. The effect of the voltage amplitude on the heatings was measured at T=77 K and f=101.5 Hz with the actuator #8114: the observed heatings as function of the square of the voltage amplitude are shown in Fig.16. These data confirm the quadratic dependence of dielectric losses on the voltage, at least for small heating (e.g., $\Delta T \leq 2$ K, $V \leq 2.1$ V). The observed departure from the quadratic dependence at higher voltage, could be attributed to nonlinear effects resulting from the dependence of Cp and sin(δ) on temperature.

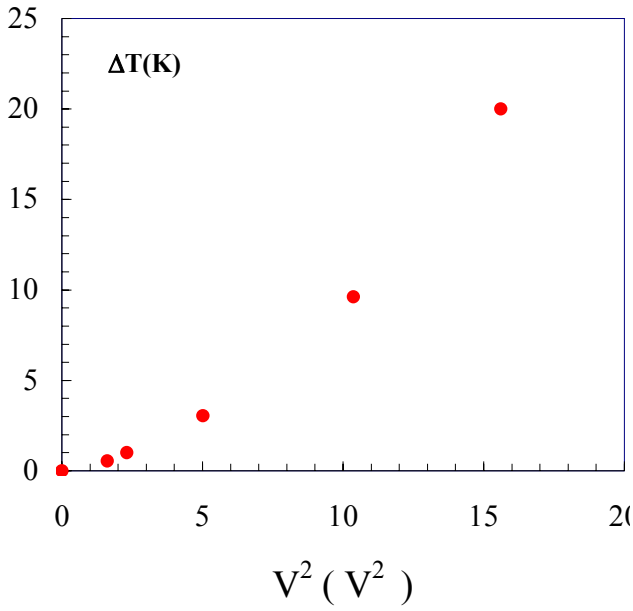

Figure 16: Heating due to dielectric losses: effect of voltage amplitude.

Conclusion

Actuators of different production series from piezosystem JENA were investigated [7]. These actuators, which are of the same type (Maximum stroke $\Delta X \approx 42$ µm @ T=300 K, calibration curve given by JENA), were rejected because of five main drawbacks and limitations:

1) Maximum stroke less than 2 µm at 2K (3 µm are required),
2) Insufficient blocking force : ~1kN @ 300K (3kN are required),
3) Low mechanical stiffness: 25N/µm (100 N/µm are required),
4) Lack of fabrication reproducibility from batch to batch (i.e. different behaviour of ΔX vs. T),
5) Very short lifetime when operated at 2 K (electrical breakdown and/or mechanical damages).

Tests results with PICMA and NOLIAC actuators

As actuators from Piezosystem JENA did not fulfil the requirements in terms of performance and lifetime for our application, we decided to study two other types of piezostacks (PICMA and NOLIAC).

Calibration: full range displacement versus temperature

In contrast to JENA actuators, these two types of piezostacks supplied by PI and NOLIAC Companies respectively are not calibrated. We used JENA actuator and the displacement sensor for their calibration (i.e., measurement of full range displacement) at room temperature. More precisely, in a first test the actuator from Piezosystem JENA is used to calibrate the displacement sensor, which in turn is used in a second step as reference for the calibration of PICMA or NOLIAC actuators. A calibration curve of a PICMA piezostacks at T≅300K is shown in Fig.17. These data show the well known hysteresis with a full range displacement of 40 µm @ V_{max}=120V. Note that this hysteresis is completely negligible for T< 4.2 K.

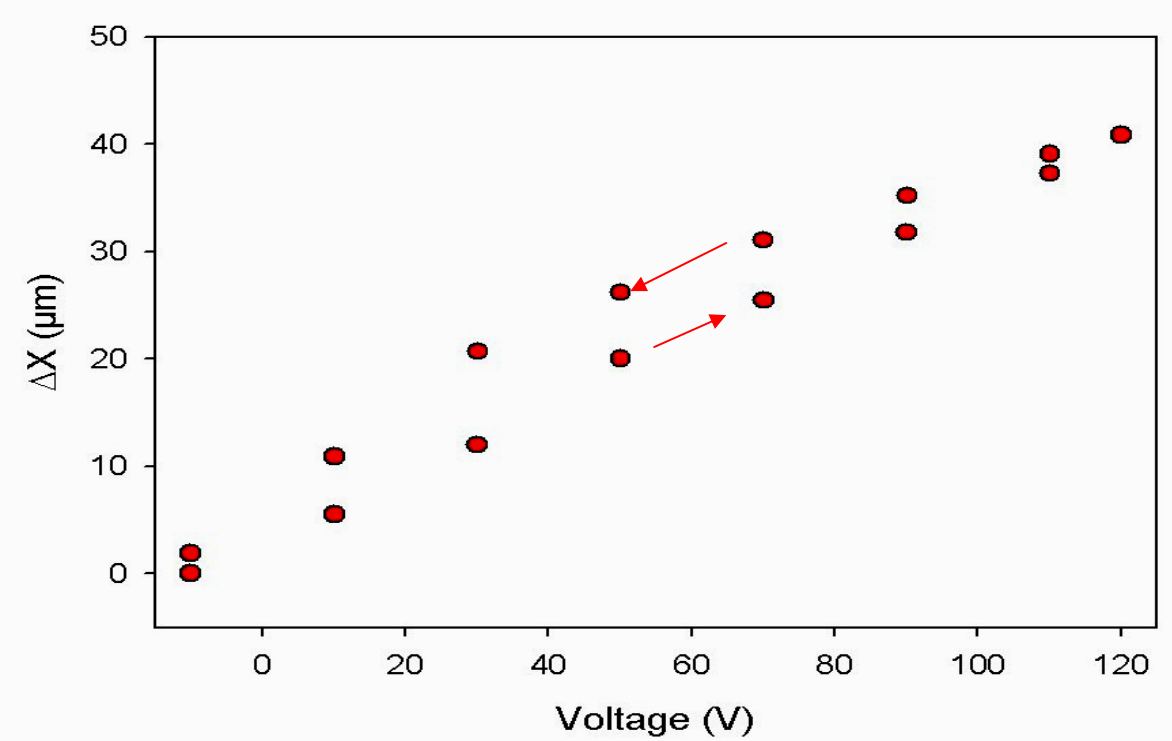

Figure 17: Calibration curve of PICMA #1 actuator à T ~300K.

It should be stressed that the maximum operating voltages of PICMA and NOLIAC actuators are respectively 120V and 200V (see Table 1). Moreover, for NOLIAC actuators due to the available electronics (Amplifier from JENA Company), the maximum available voltage is 150V and this value is much lower than the maximum operating voltage. The measured variations of the full range displacement for PICMA and NOLIAC actuators with temperature are compared in Fig. 18.

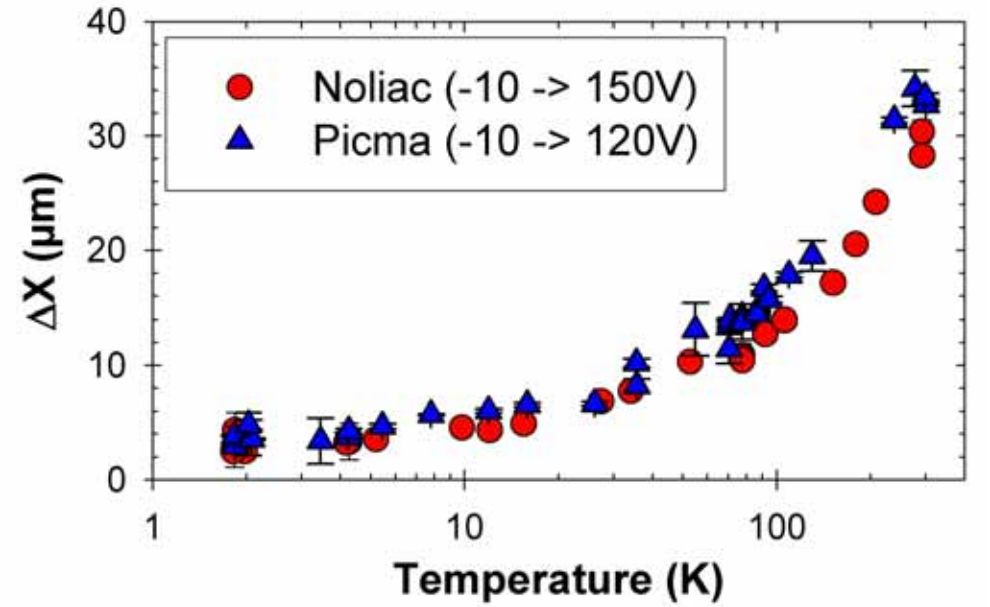

Figure 18: Full range displacement versus temperature of PICMA and NOLIAC piezostacks.

The two curves of Fig. 18 have a similar shape. Moreover, these data show a non linear behaviour: the slope of ΔX vs. T decreases strongly with temperature. The full range displacement is decreased strongly with T from ~40 µm @ T=300 K down to ~3 µm @ T=2K: this decrease by a factor of ~13 when T is lowered from 300 K down to 2 K is in the range of values reported previously by other authors [7-9]. For actuators of PICMA and NOLIAC type, the measured full range displacement is ΔX=2.8µm-3µm at T=2K, which corresponds to the required detuning compensation Δf≈1kHz for TESLA nine cells cavities operated at E_{acc}=33 MV/m. Moreover, this non linear behaviour of ΔX vs T, already observed previously [7-13] is tightly correlated to the strong dependence of the actuators parallel capacitance Cp on temperature as illustrated in Fig. 19.

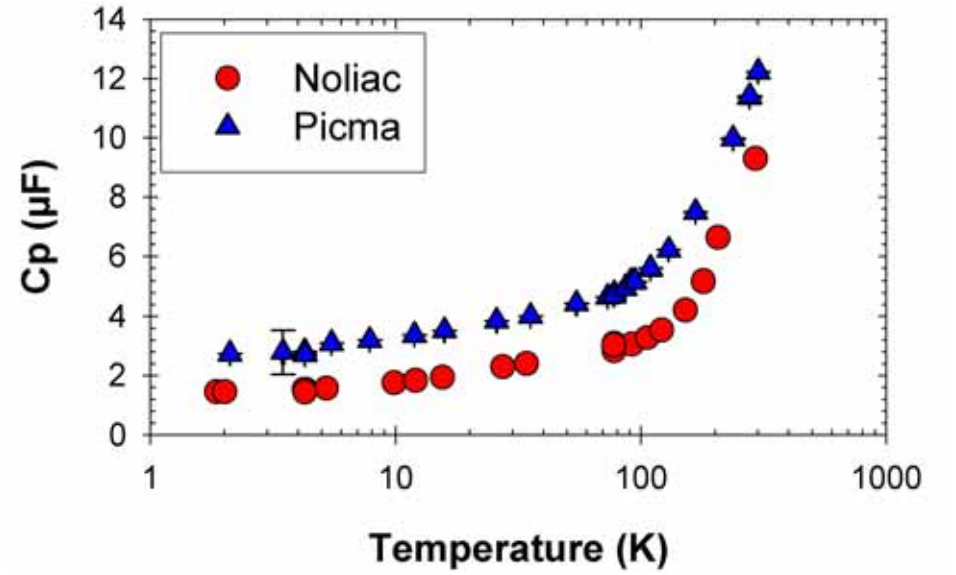

Figure 19: Capacitance versus temperature for PICMA and NOLIAC piezostacks.

Furthermore, the strong correlation between the full range displacement ΔX and the parallel capacitance is clearly observed in Fig. 20: at low temperature (i.e. T≤100 K), we notice a linear relationship between ΔX and C_p (i.e. $\Delta X \propto C_p$). This behaviour, which is similar to that observed for piezostacks from Piezosystem JENA [7], gives a straight-forward mean to calibrate actuators. Indeed, capacitance measurements are simpler and less time consuming, as compared to a true calibration (i.e., ΔX vs. T) and especially for a large number of actuators (e.g., ~1000 for XFEL).

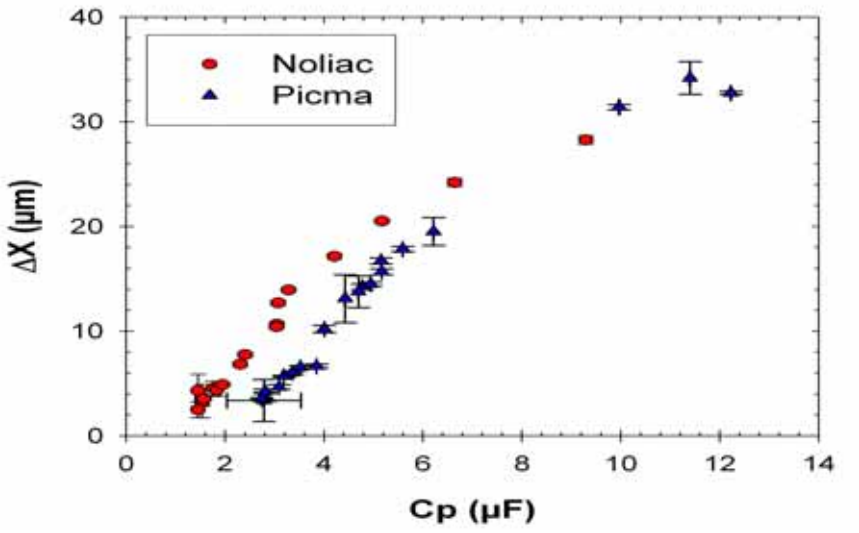

Figure 20: Full range displacement versus capacitance for PICMA and NOLIAC piezostacks.

Dielectric and thermal properties

Measurements of the following parameters were automatically performed for T ranging from 1.8K to 300K: a) dielectric properties (Cp, complex impedance: Z, and tg(δ) @ 100Hz, 120 Hz and 1kHz), heating ΔT vs. sinusoidal voltage amplitude V_{mod} and frequency f, b) thermal properties (Specific heat: C_{th}, thermal resistance: R_{th} and time constant $\tau = R_{th}.\ m.C_{th}$, with m: actuator mass).

a) Capacitance and dielectric constant versus T

The effect of temperature on the capacitance Cp was already presented in a previous section. The dielectric constant ε_r of the material vs. T, which is deduced from Cp, is obviously homothetic to the curve of Fig. 19: for PICMA actuators ε_r decreases from 1454 at T=300K to 328 at T=1.8K.

b) Loss factor and parallel resistance

The variations of loss factor with temperature are shown in Fig. 21. Again, in contrast to the parameters ΔX, Cp and ε_r, the loss factor (i.e., tg(δ)) did not show a monotonous dependence as function of temperature: from its room temperature value, tg(δ) increases as T is decreased then reach a maximum afterwards it decreases as T is lowered down to 1.8 K.

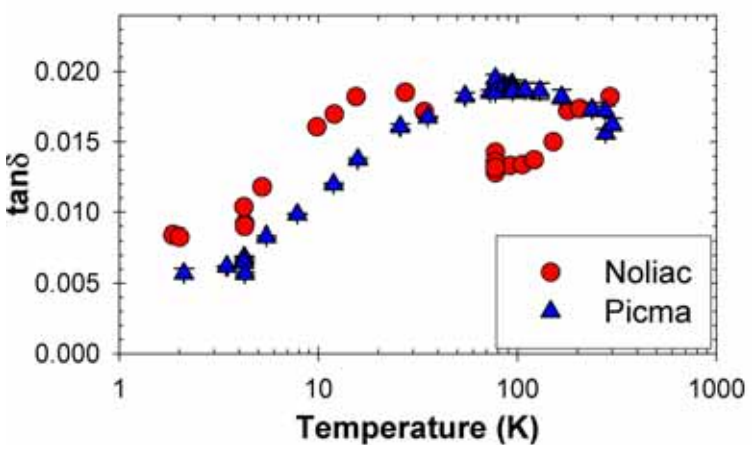

Figure 21: Variations of loss tangent with temperature.

The loss factor experimental data obtained with the three types of actuators (JENA, PICMA and NOLIAC) show that such behaviour (i.e., existence of peak in tg(δ) vs. T curve) is common to all these actuators. However, the exact shape of the curve and the location of the peak of the loss factor depend on the supplier: it could be attributed to the piezoelectric material chemical composition, the lattice structure and the fabrication process. The peaks are located around T≈20K and T≈90K for NOLIAC and PICMA piezostacks respectively.
As shown in Fig. 22, the parallel resistance Rp increases exponentially when the temperature is decreased. It should be emphasized that a high value of Rp corresponds to a low leakage current, resulting in a better insulation quality and increased lifetime of the actuator. Note that for actuators supplied by Piezosystem JENA, we systematically observed a dramatic decrease of Rp (e.g., Rp<1Ω) when the electromechanical breakdown occurred.

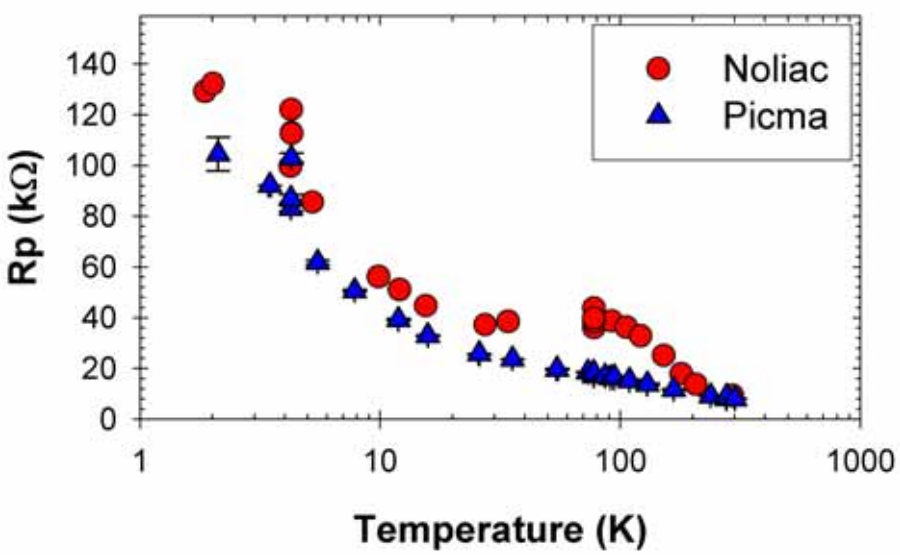

Figure 22: Parallel resistance versus temperature.

c) Dielectric and thermal properties

For an initial temperature of the piezostacks T_0=1.8K, the dielectric heating ΔT versus time of a PICMA actuator subjected to a sinusoidal voltage is shown in Fig. 23. In this test, the amplitude and the frequency of the modulation voltage are respectively V_{mod}=1.5 V.

These data clearly show an exponential dependence of the heating on the time t namely, $\Delta T = \Delta T_{max}.(1-\exp(-t/\tau))$. The fit to the experimental data leads to the following values of the different parameters: τ=376 s, $R_{th}=9.10^{5}$mK/mW and $m.C_{th}=4.310^{-4}$ J/K.

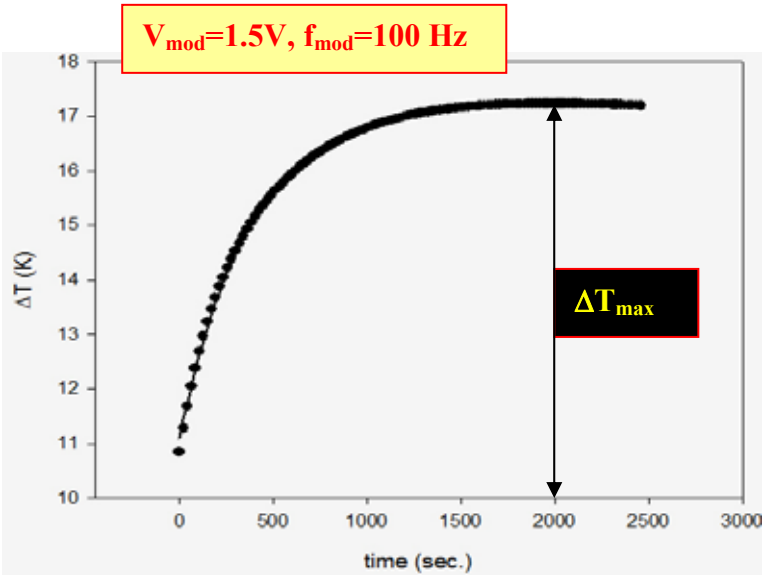

Figure 23: Dielectric heating ΔT of the actuator at T=1.8 K.

Notice that an amplitude V_{mod} =1.5 V corresponds to a displacement of 170 nm of the cavity wall (i.e., frequency shift Δf=68 Hz); the resulting total dielectric losses and steady state heating are respectively P_{diel}= 20 µW and ΔT_{max}=17 K. Finally, the steady-state heating ΔT vs. modulation voltage amplitude and frequency is shown in 3D plot of Fig. 24. The observed steady-state heating (i.e., $\Delta T=R_{th}.P_{diel}$) is well described by the well-known expression of the total dielectric losses P_{diel} (i.e., $\Delta T \propto P_{diel} = \pi.f.Cp.V_{mod}^{2}.\sin(\delta)$). Notice again that the small departure from the quadratic dependence observed at high modulation voltage amplitude and/or frequency, is attributed to nonlinear effect resulting from Cp and sin(δ) dependence on temperature.

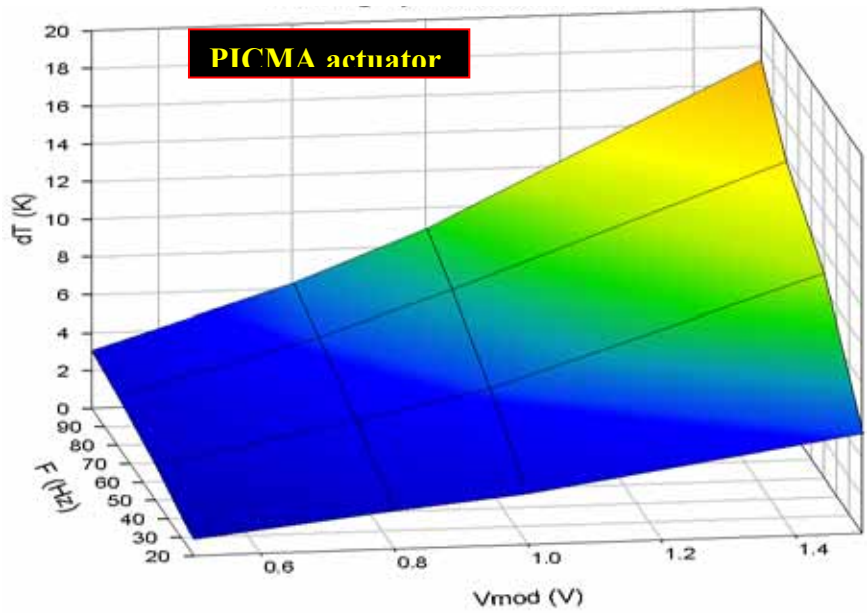

Figure 24: 3D plot of heating versus modulation voltage amplitude and frequency.

Preloading experiment

In order to provide for a reliable operation of the accelerator, the piezoelectric actuators (e.g., 40.000 units for ILC) should function satisfactorily for a period close to machine life duration (~20 years). The corresponding actuator lifetime requirements should be much higher than 3.210^9 cycles (pulsed mode, repetition rate: 5 Hz). Moreover, previous studies showed that the life time of piezostacks depends strongly on the applied preloading pressure P_{Load} (Fig. 25) with an optimum value P_{Load}~100Bars at T=300 K. On the other hand, the actuator displacement versus preloading pressure characteristics (Fig. 26) is not monotonic: the maximum displacement is observed for P_{Load} in the range 20MPa- 50MPa [14]. Further, our observations from the tests of actuators from Piezosystem JENA in particular, show that the lifetime versus preload curves depends strongly on actuator material and fabrication process.

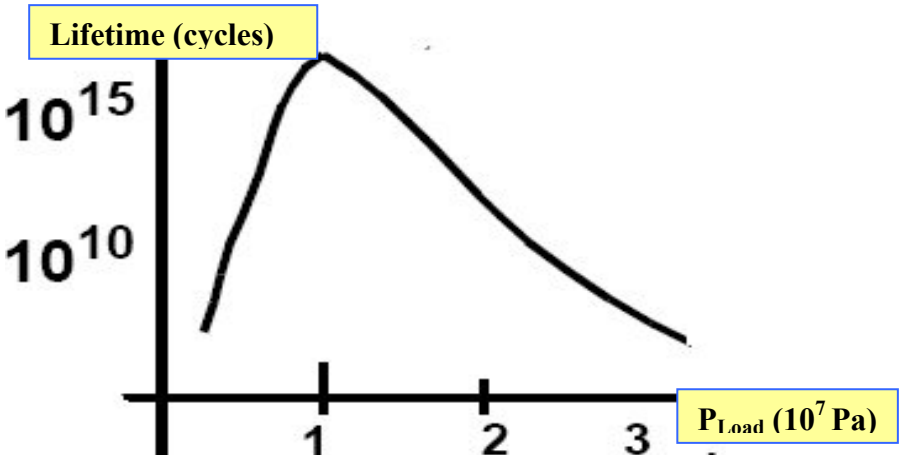

Figure 25: Sketch of lifetime versus preloading pressure.

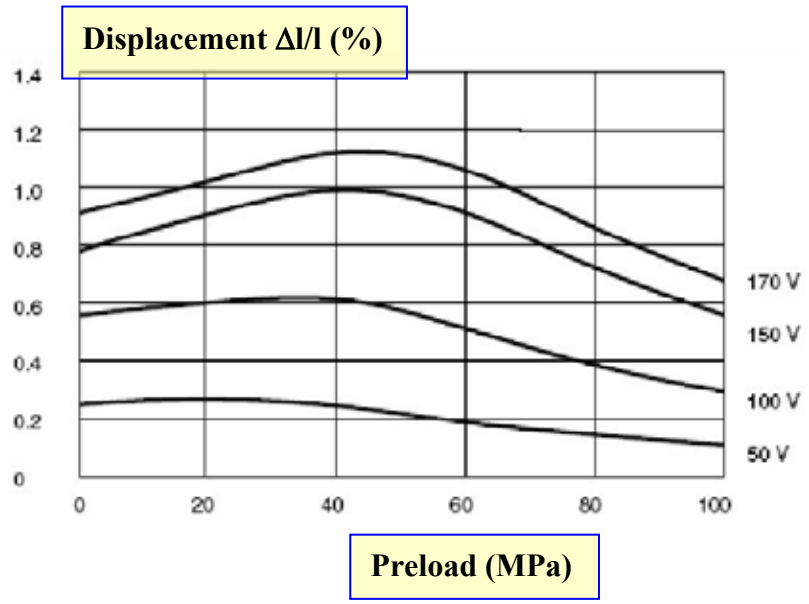

Figure 26: Relative displacement versus preloading pressure at different voltages *(R. Binding et al., see ref. 14).*

Due to the lack of data concerning piezostacks used under the operating conditions in the actual tuner (i.e., under vacuum and cryogenic conditions), it is necessary to perform an experimental investigation of electromechanical behaviour of actuators subjected to axial preload at cryogenic temperature.

Description of test apparatus

The main goals of the experiment are the following: 1) Study the effect of a variable and controllable axial preload on the electromechanical properties of the piezoelectric actuator (stroke, capacitance, loss factor, impedance, etc), 2) Development of a procedure for applying, adjusting and controlling the preload, 3) Study of the behaviour of piezostacks as force sensor, 4) Measurement of the mechanical stiffness of the actuator. The apparatus should allow to applying and measure a controlled and adjustable axial force in the range 1kN- 4kN to the piezoelectric actuator. Moreover, the piezoelectric actuator should be subjected to this force in an environment similar to the operating conditions in the tuner, namely under vacuum (pressure<10^{-5} mbar) and at cryogenic temperatures. We have designed and constructed an apparatus dedicated to low temperature preloading experiment [15-16]. The simplest way for applying a vertical downward compressing force is naturally to use gravity. But due to the relatively high value (~100 kg) of the mass (in case of direct load on the actuator axis) needed for achieving force of ~1kN, it is obvious that a lever arm system with a magnification factor ~10-15 (lever arms ratio) should be used. A diagram of the operating principle of the method is presented in Fig. 27. The piezostacks to be tested is enclosed in a stainless steel vacuum chamber, which will be immersed in a liquid helium bath. A rotating arm located at room temperature (T~300 K) outside the cryostat allows applying a vertical downward force (along the actuator axis) to the piezostacks via a high stiffness transmission rod. The preloading force applied to the actuator is simply adjusted by varying the load at the extremity of the rotating arm. At the mechanical equilibrium, the sum of the momentums of all the forces is equal to zero. Assuming a negligible friction on the rotation axis, the preloading F force is simply given by the law of conservation of angular momentum:

$$F = Fc \cdot \left(\frac{L_C}{L_P} \right) + m_A \cdot \left(\frac{L_A}{L_P} \right) \cdot g \qquad (3)$$

Where m_A is the masse of the rotating arm, L_P, L_A and L_C are respectively the distances from the rotation axis of the piezostacks axis (L_P), the centre of mass of the arm (L_A) and the loading mass (L_A) and g the gravity constant.

Taking into account the available space on the upper flange of the cryostat insert, which support vacuum pumps and other components, the values of the lengths L_P, L_C are respectively 30mm, 430mm leading to a lever arm ratio $r=L_P/L_C=14.66$. The key element of the preloading system is the rotating arm; consequently it was carefully designed using Finite Element Method numerical simulations [17] in order to verify that it behaves as a rigid body. Note that the simulation model includes the transmission rod and the actuator.

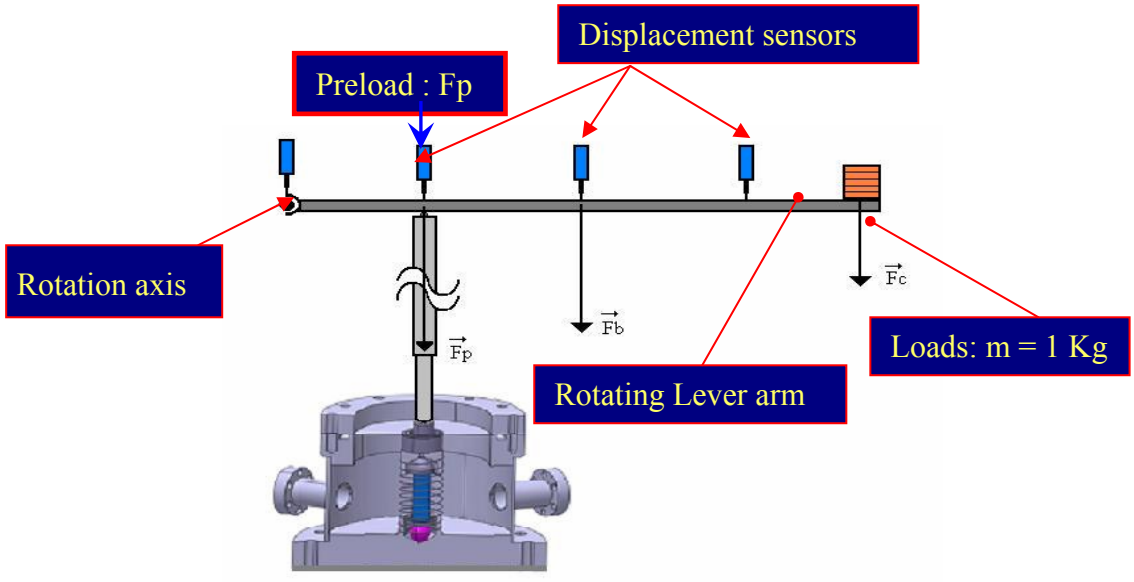

Figure 27: Diagram of the operating principle of the method.

The geometries of the different arms studied and the main results concerning their mechanical behaviour are listed in Table 2.

Table 2: Mechanical characteristics of the rotating arms studied .

Cross-section Shape	**Dimensions** (mm^3)	***Material***	**ΔXp (μm)**	**ΔXc (mm)**	**ΔXc /ΔXp**	**Bend (mm)**
Rectangle	40x10x500	*Aluminium*	66.1	27.5	416	26.5
Rectangular tube	20x20x500 (wall thick.: 2mm)	*Aluminium*	66.4	12.4	186	11.4
Square	45x45x500	***Stretched steel***	59.4	0.91	**17.7**	0.043

The computed displacements for the square shape cross-section arm made of stretched stainless steel lead to a ratio ΔXc/ΔXp=17.7 for the vertical displacements at the masse location and along the piezostacks axis respectively. This figure is close to the value of lever arm ratio $r=L_P/L_C$ =14.7: the relative difference (i.e., 20%) is due to the finite rigidity of the arm. As expected, due to their low stiffness, the first two aluminium arms of rectangular cross-section shape don't behave as a rigid body. More precisely, they show a high deflexion or bending resulting in a ratio ΔXc/ΔXp one order of magnitude higher than the target r=14.7. Furthermore, the actuator is housed in an evacuated chamber with a removable thin end plate as detailed in a previous section. The operating principle of this device is the following: 1) actuator mode: a voltage is applied to the piezoactuator which expand leading to a deformation of the upper thin sheet; the resulting motion is transmitted to the displacement sensors at 300 via a Φ16 stainless steel rod, 2) Force sensor mode: a loading force is force is applied to the piezostacks via de transmission rod and the response of the actuator (i.e., capacitance and transient voltage) is measured. A close view to the upper part of the preloading system is shown in Fig. 28.

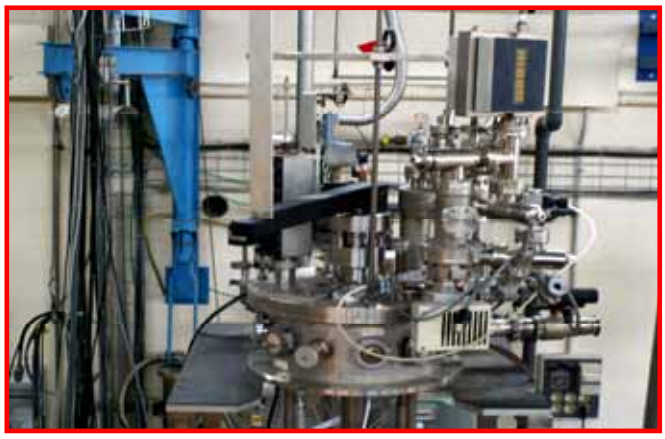

Figure 28: Photograph of the upper part of the insert ready for cryogenic test.

Experimental results and discussion

Repeatability test at T=4.4K

The sensitivity of a PICMA type piezostacks to a preloading axial force at cryogenic temperature was investigated. The variations of the relative capacitance $\Delta Cp = Cp - Cp_0$, with reference to the capacitance Cp_0 of the actuator when it is subjected to the arm preload F_0=733 N only, as function of the preloading force F at T=4.2K are shown in Fig. 29. In order to measure the repeatability of the experimental data, two runs were performed for F increasing from 0 up to 4 kN.

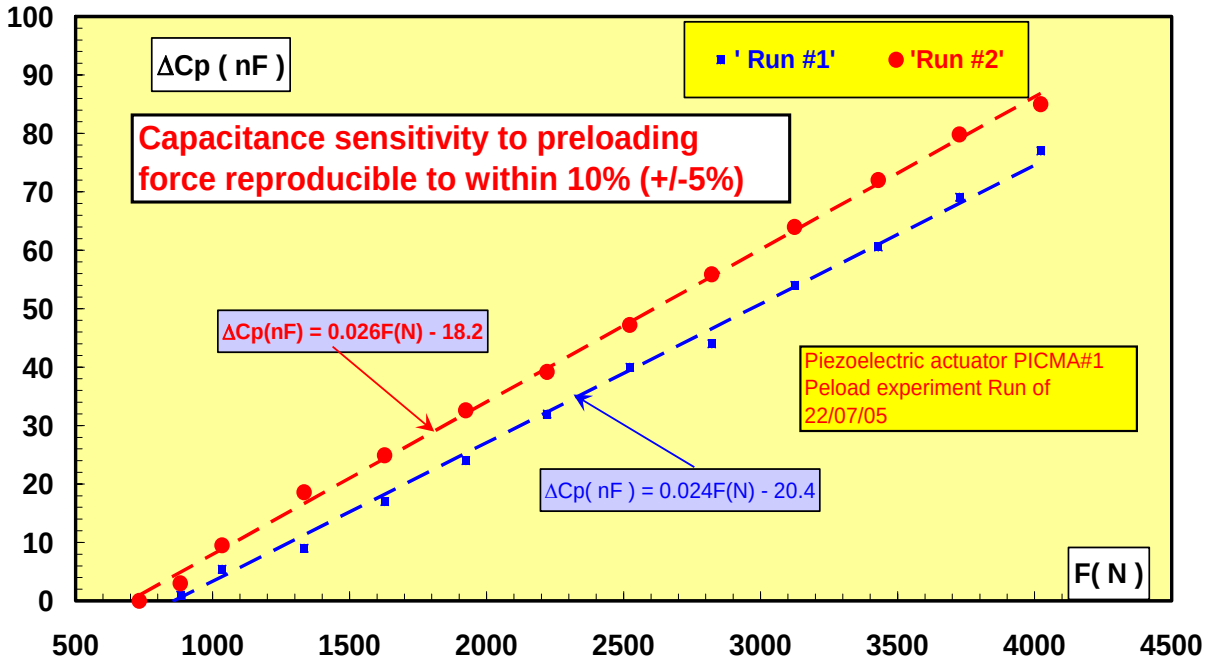

Figure 29: Sensitivity to preloading at T=4.4 K (Repeatability test), Cp_0=3.134 µF.

The data show a linear behaviour of ΔCp vs. F. Moreover, we observe a good repeatability: the relative variation of the slope ΔCp/ΔF=25nF/kN at T=4.4K for F increasing from 0 to 4kN between the two runs performed is ±5%.

Sensitivity to preloading at T=2.05K

The sensitivity of the actuator to preloading was measured at T=2.05 (T=2 K: ILC operating temperature) for increasing and decreasing load (Fig. 30). Non linear effects are observed at low preloading force when F is increased from zero to ~1.3 kN: these effects are due to friction, stick-slip among non linear phenomena in the preloading device mechanism (rotating arm, bellows). Further, these data clearly show a large hysteresis for increasing and decreasing the preloading force. This hysteretic behaviour, which is similar to that observed in displacement versus voltage characteristics, could be attributed to the intrinsic irreversibilities in the piezoelectric material itself.

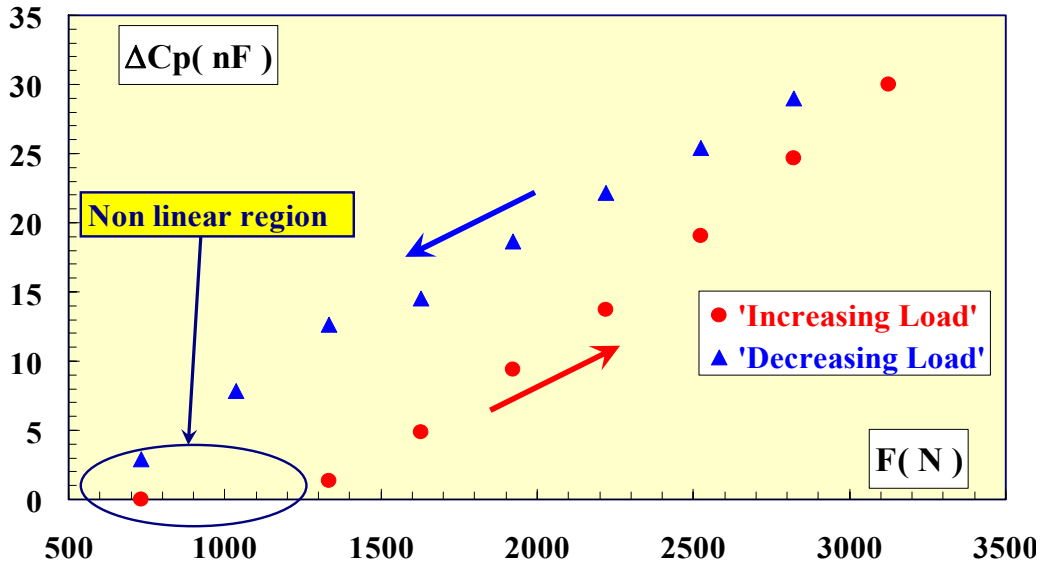

Figure 30: Capacitance versus preload at T=2.05 K, Cp_0=2.879 µF.

Finally at T= 2.05K, the measured sensitivity to preloading are 16nF/kN (respectively 10nF/kN) for F increasing (respectively decreasing).

Effect of temperature on the sensitivity to preloading

We investigate the effect of the actuator temperature on its sensitivity to preloading. Systematic measurements [15-16] of ΔCp vs. F were performed for T in the range 1.7 K-300K. These results clearly show a linear dependence of the capacitance variation, at a given temperature, with the applied preload in the whole temperature range. Further, the non linear effects observed at T= 2K and low preloading force, were confirmed for all temperatures. Moreover the sensitivity to preloading, in the linear region, depends strongly on the temperature as illustrated in Fig. 31. Each datum point of this curve is simply the slope of the curve ΔCp vs. F at a given temperature.

More precisely, ΔCp/ΔF shows exponential dependence on temperature: for increasing preload mode, ΔCp/ΔF increases with T from 16nF/kN at T=2 K to 426nF/kN at T=300 K.

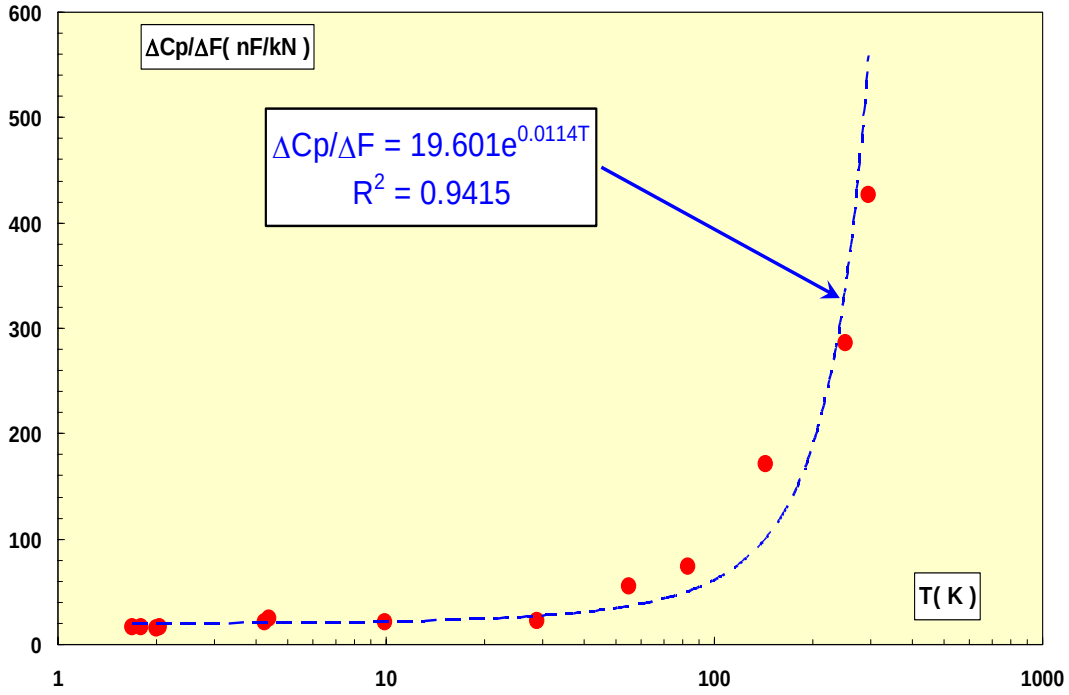

Figure 31: Sensitivity to preloading versus temperature for a PICMA actuator.

Piezostacks as dynamic force sensor

The behaviour of the piezostacks as dynamic force sensor was also studied. The transient response of the actuator to various negative and positive steep preloads variations ΔF=±nx150 N (n=1, 2, 3) was recorded at T=4.2K (Fig. 32-Fig. 33). The results call for the following remarks: 1) a steep voltage increase (capacitor charging) followed by an exponential decrease (capacitor discharging) is observed, 2) the peak actuator voltage ΔV_p is repeatable (3 %).

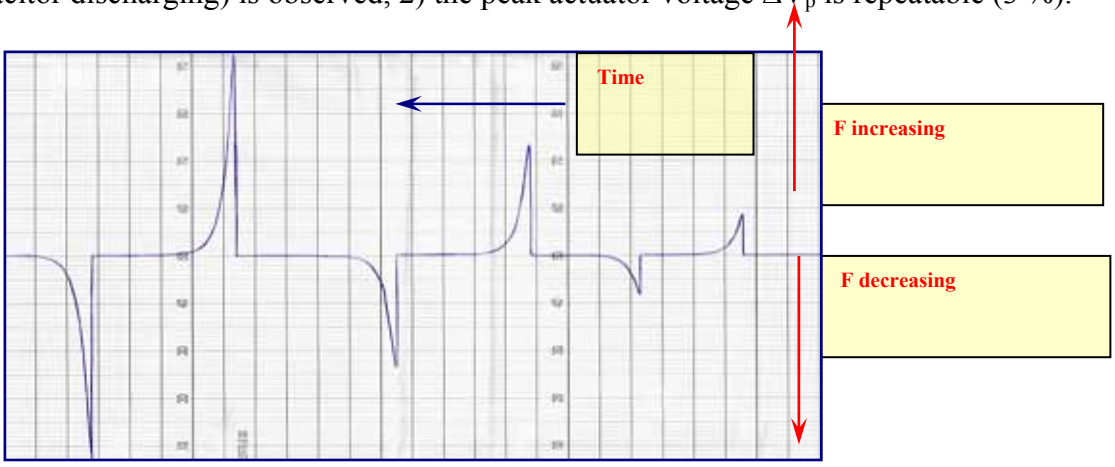

Figure 32: Transient response of a PICMA type actuator to various steep preload variation ΔF=±nx150 N (n=1, 2, 3) at T=4.2 K.

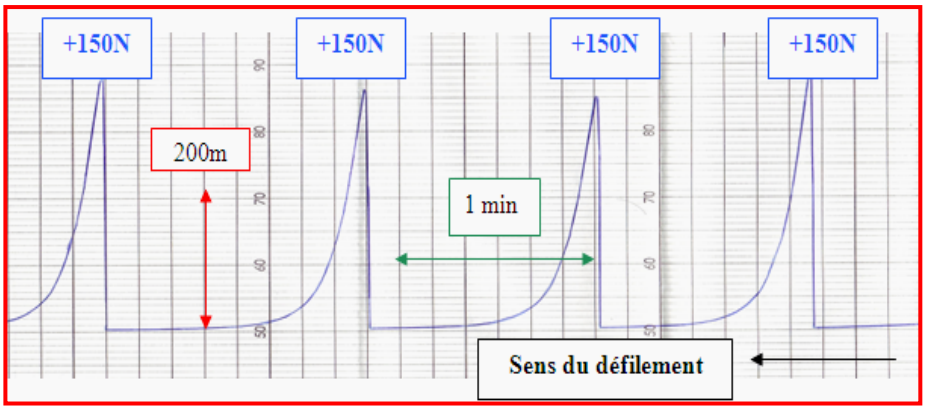

Figure 33: Transient response of a PICMA type actuator to a steep preload variation ΔF=150 N at T=2 K: repeatability tests.

The experimental data of Fig. 32-Fig.33 show the reversibility and the linearity of the response: the peak voltage is proportional to preload variation ($\Delta V_p \propto \Delta F$) and change de sign with ΔF. This behaviour is clearly illustrated in Fig. 34-Fig.35

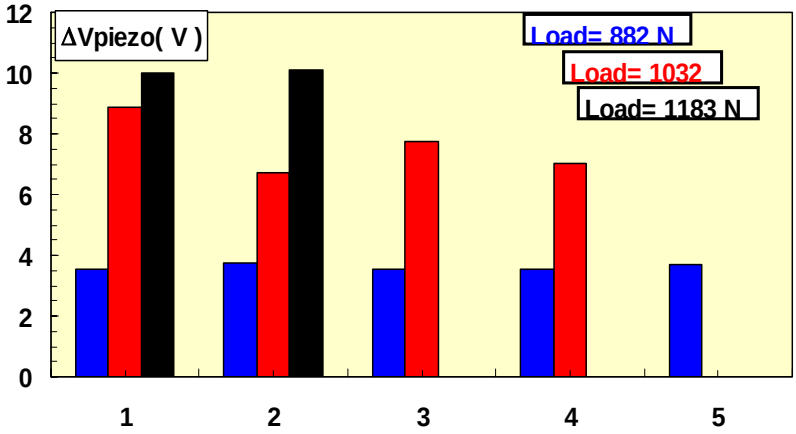

Figure 34: Histogram of the peak voltage recorded during transient response of the actuator to various steep preload variation ΔF=±nx150 N (n=1, 2, 3) at T=4.2 K.

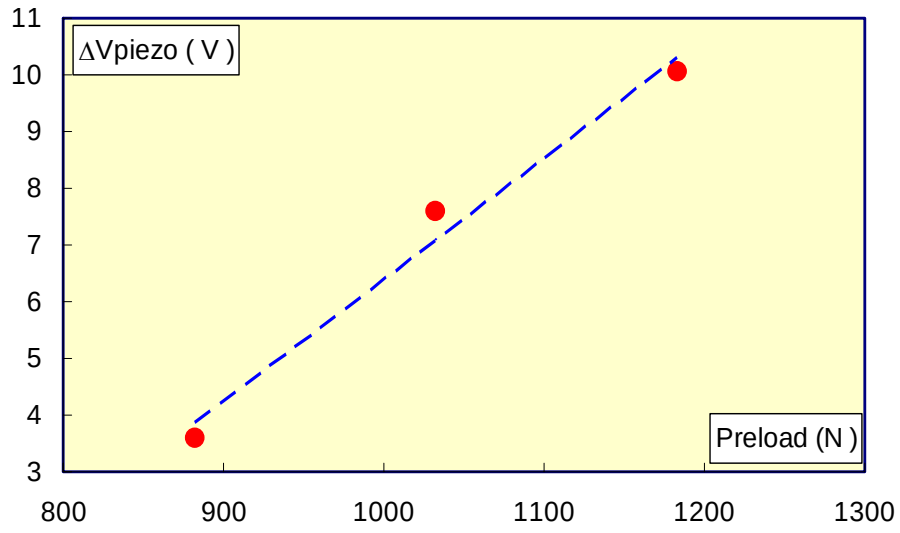

Figure 35: Peak voltage versus preload at T=4.2 K.

Effect of fast neutrons radiation at cryogenic temperatures

An experimental program, aimed at investigating the effect of fast neutrons radiation on the characteristics of piezoelectric actuators at liquid helium temperature (i.e. T~4.2 K), was proposed for the working package WP#8 devoted to tuners development in the frame of CARE project. A neutrons irradiation facility, already installed at the CERI cyclotron located at Orléans (France), was upgraded and adapted for actuators irradiations tests purpose. A deuterons beam (maximum beam energy and beam current: 25 MeV and 35µA) collides with a thin (thickness: 3 mm) beryllium target producing a high neutrons flux with low gamma dose (~20%): a neutrons fluence of more than 10^{14} n/cm^2 is achieved in ~20 hours of exposure. A dedicated cryostat was developed at IPN Orsay and used previously for radiation hardness test of calibrated cryogenic thermometers and pressure transducers used in LHC superconducting magnets. This cryostat could be operated either with liquid helium or liquid argon. This irradiation facility was upgraded for allowing fast turn-over of experiments and a dedicated experimental set-up was designed, fabricated, installed at CERI and successfully operated for radiation hardness tests of several piezoelectric actuators at T~4.2 K [18]. This new apparatus allows on-line automatic measurements of actuators characteristics and the cryogenic parameters. Further, the test-cell and actuators are equipped with high purity Ni foils for measuring the total neutrons dose by an activation method. More details of the irradiation test facility will be found in a separate report [18].

Overview of the test facility

The fast neutrons irradiation test-facility at low temperature is similar to that used previously for the radiation hardness test program dedicated to the evaluation of various cryogenic sensors for LHC projects (thermometers, pressure sensors,…[19-21]). More precisely we use the same cryostat (Fig. 36).

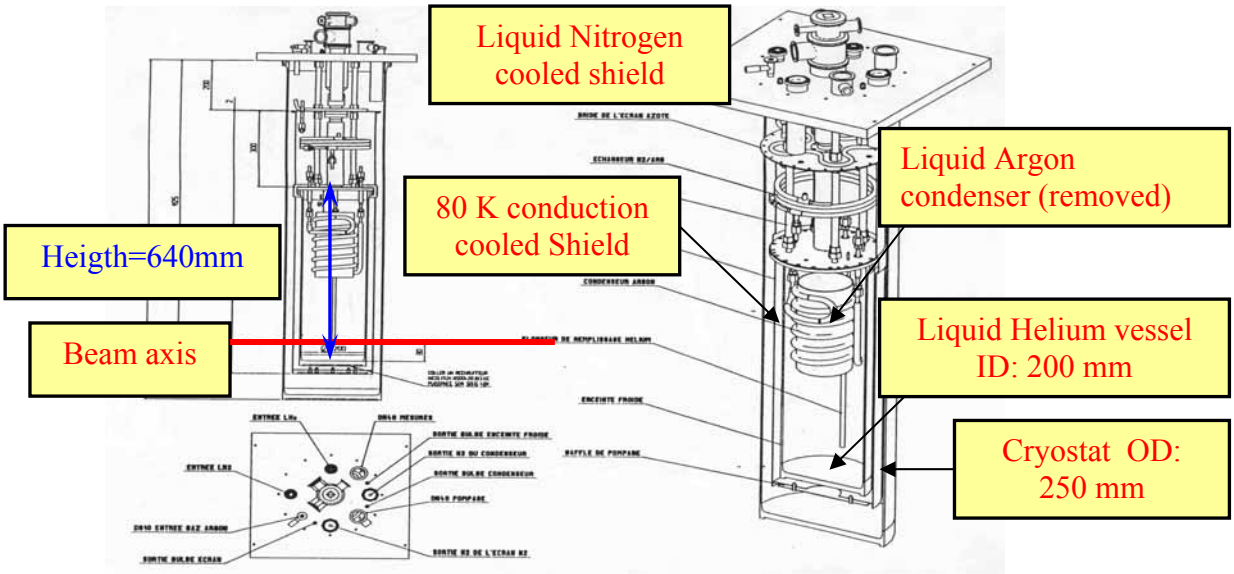

Figure 36: Drawing of the cryostat and the insert

The internal diameter and available height for the cryogenic liquid (i.e., helium or argon) vessel are respectively 200 mm and 640 mm. The vacuum vessel and the parts of the insert located in the neutrons beam region are made of aluminium to avoid material activation. Note that the argon condenser, which is not used for the actual liquid helium tests, was removed. Due to the relatively small available space in front of the beam line, we have designed and installed a handling system (Fig. 37) consisting of a support sliding in a horizontal rail. This system allows the following operation: a) moving easily and rapidly the cryostat, b) positioning the cryostat and adjusting the location of the test-cell in front of the beam line.

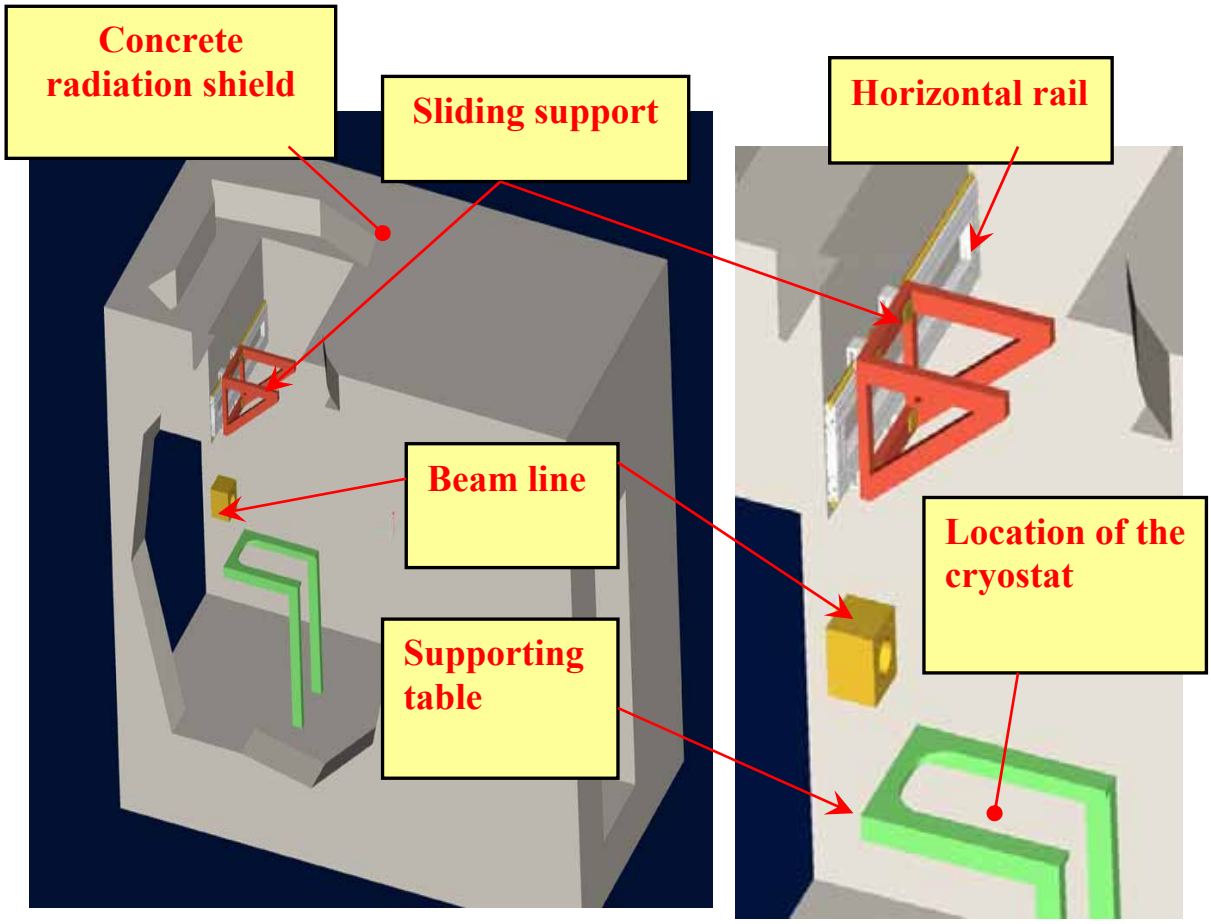

Figure 37: 3D view of the cryostat handling system in front of the beam line.

The actuators to be simultaneously irradiated (up to four) are housed in vacuum can, which is immersed in a liquid helium bath for low temperature experiments at T~4.2 K. The cryostat is placed behind a 3 mm thick beryllium target located at a distance d=20 mm -30 mm from the cryogenic vessel. The high flux of neutrons is produced by the collision of a deuterons beam (maximum energy and intensity: 25 MeV and 35μA respectively) with the beryllium target using the break-up reaction $^{9}Be(d, n)^{10}B$. The diagram of the process for the production of fast neutrons is shown in Fig. 38. Note that the target is water-cooled (forced convection) in order to avoid strong heating of the material.

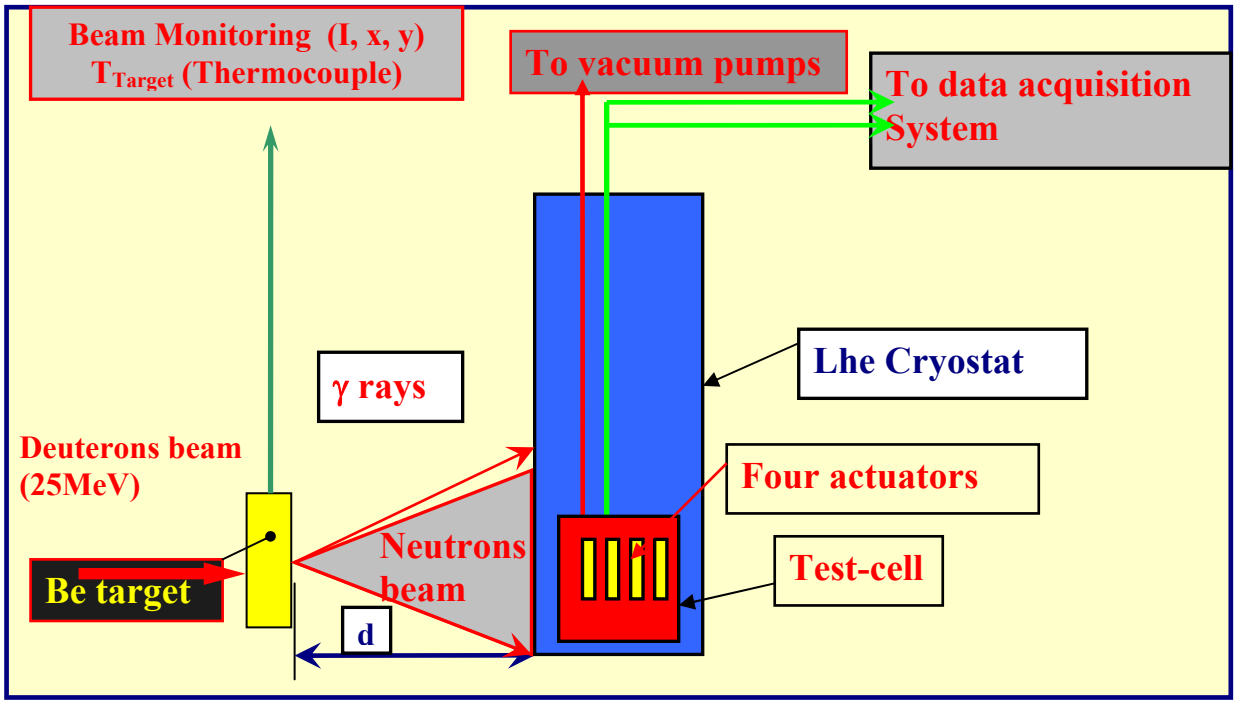

Figure 38: Sketch of fast neutrons production process.

Description of the experimental set up

The test-cell

As the actuators will not operate in the same conditions as the LHC thermometers, a new insert was developed for actuator irradiations tests. In fact, for their operation in the fast cold tuning system of SRF cavities, the actuators are located in the insulation vacuum of the cryomodule and are not directly cooled by superfluid helium. The main design requirements of the test-cell are listed in Table 3.

Table 3: Design requirements of the irradiations test-cell

Component, parameter (Unit)	**Design value- Material**
All component in cold area	**Suitable for operation in radiation and cryogenic environment**
Chamber and actuator support	**Aluminium**
Temperature range **(K)**	**4.2 -300**
Pressure in the chamber **(Torr)**	**$<10^{-6}$**
Irradiated area (**mm^2**)	**>80x40**
Liquid Helium Pressure **(Bar)**	**1**
Liquid Helium Temperature **(K)**	**4.2 K**
Low temperature Vacuum seals	**Demountable Indium gasket**
Pumping speed in the tube **(l/s)**	**0.05**
Leak rate at T=300 K (**$mBar.l.s^{-1}$**)	**$<10^{-9}$**
Pumping time from 10^{-2} Torr to 10^{-6}Torr **(min.)**	**<10**

The test-cell (Fig .39), made of aluminium, consists mainly of a mechanical support for the actuators and a vacuum chamber with a vertical (I.D:16 mm) pumping line. The actuators are housed into the aluminium support which is inserted in the vacuum chamber. The main dimensions of the test cell are: a) internal diameter Ø100, b) actuator supports outer diameter Ø160. A high purity indium gasket is placed in a groove machined in the actuators support to insure the vacuum-tightness between the evacuated chamber and the surrounding Liquid Helium (LHe) bath. Note that a high purity (99.99%) indium gasket (wire diameter: 1mm) was used in order to reduce material activation due to exposure to radiation (See next section). Moreover, the pumping tube has two other functions: a) feed through for all the wires attached to the actuators, b) mechanical support attaching the test-cell to the cryostat insert. Each of the four piezoelectric actuators to be tested is equipped with a calibrated (temperature range: 1.5 K-300 K) resistive Allen-Bradley thermometer. The Allen-Bradley thermometers were chosen according to several criteria: 1) they feature good sensitivity and precision in temperature range of interest, 2) they are suited for use in radiation environment and the effect of fast neutrons on their thermometric characteristics is well-known [19-21].

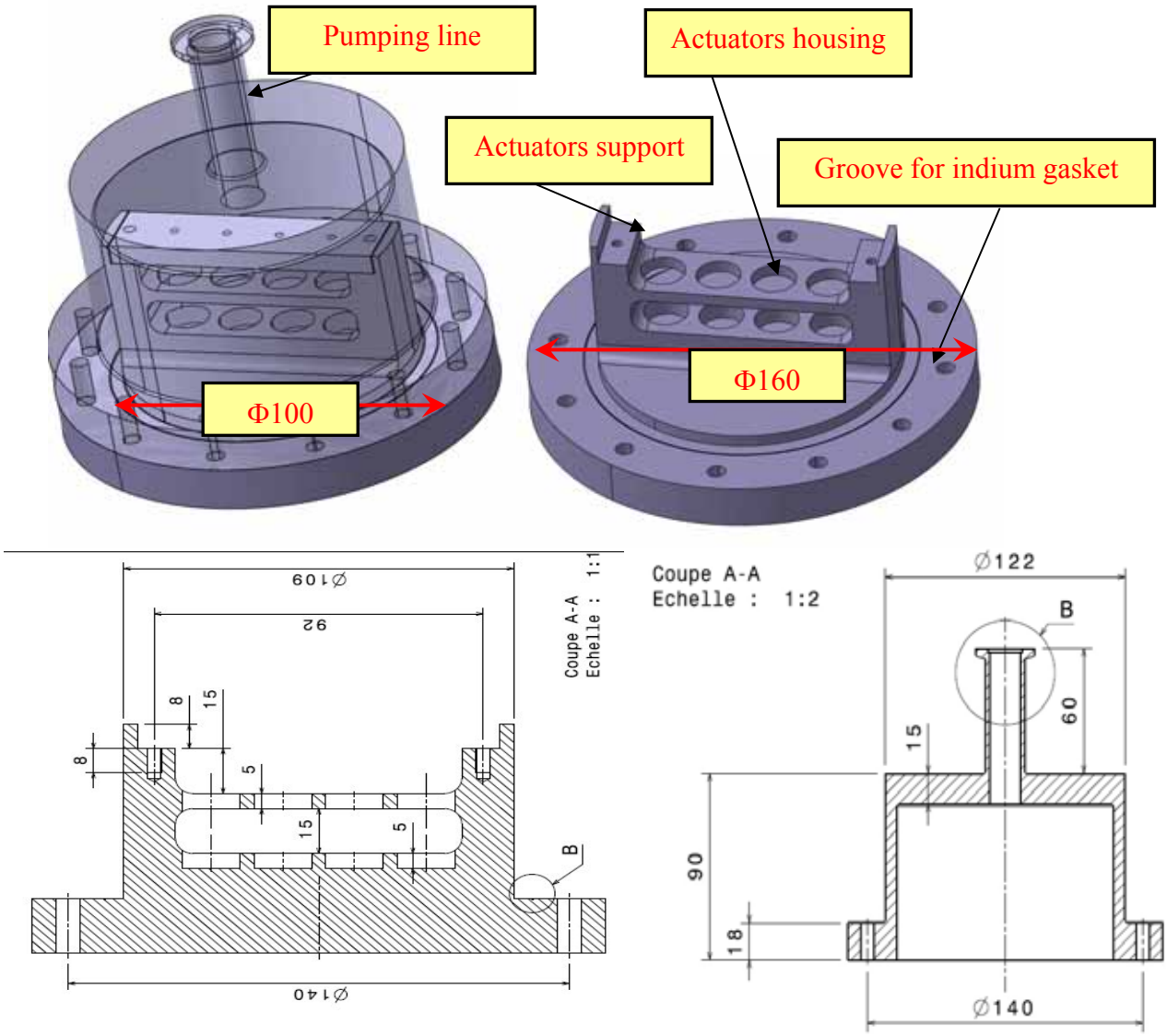

Figure 39: Drawings of the test chamber

The piezostacks are inserted into their fixture and mounted with a copper-beryllium spring on their upper extremity. Moreover an indium foil is sandwiched between the actuator lower extremity and the support in order to improve the thermal contact. Further a heater and a copper thermal anchor are attached to each actuator. The results lead to an effective tube diameter of ~8 mm to fulfil the test-cell vacuum requirements.

The piezoelectric actuators irradiated

Three types of low voltage multilayer piezostacks were subjected to irradiation tests. The main electromechanical properties of these actuators were already given in a previous section. Notice that the irradiation tests data concerning piezostacks from Piezosystem JENA will be not included in this report. They were tested for historical reasons (first actuators used in the cold tuner of TTF cavities) but these actuators are not good candidate for the tuner: their life time is very short at cryogenic temperatures. Three to four actuators of each type will be tested simultaneously to improve the statistics.

Neutrons spectrum and irradiation calculations

The material used for the construction of the cryostat insert should be suitable for operation in radiation and low temperature environment. Hence it should be chosen according to activity considerations and cryogenic performance (e.g., low thermal conduction). More precisely the activations of the following materials were calculated: 1) indium for gasket, 2) aluminium (vacuum chamber, actuator support and pumping line) and 3) other materials (screws, nuts among others). The maximum energy E_{max} and intensity I_{max} of the deuterons beam delivered by the CERI cyclotron are respectively 25 MeV and 35 μA. Further, the envelop size of the beam is 5x5 mm^2. The neutrons are produced by the collision of the deuterons beam with a 5 cm thick beryllium target located in front of the cryostat: the resulting distance between beryllium target and actuators support is in the range 15cm-30 cm. The neutrons production process is based on the break-up reaction $^{9}Be(d, n)^{10}B$.

Neutrons spectrum

The expected spectrum of these neutrons will be similar (homothetic) to that obtained with SARA facility [22] with a magnification due to the differences in the values of the maximum energy of the deuterons beam (E_{max} =25 MeV for CERI facility, E_{max} =21 MeV for SARA facility). The validity of this approximation is well confirmed by the work of Parnell [23] and Maunoury [24]. Maunoury showed that the mean energy $<E_{neutrons}>$ of the neutrons spectrum in the beam direction increases linearly with the deuteron energy E_d according to the following empirical relation ship:

$$< E_{neutrons} >= 0.38E_d + 0.57 \quad (4)$$

The expected spectrum is calculated by using the spectrum measured at SARA facility, which is interpolated for a 25 MeV deuteron beam and normalised at the integrated dose: the corresponding curve are shown in Fig. 40.

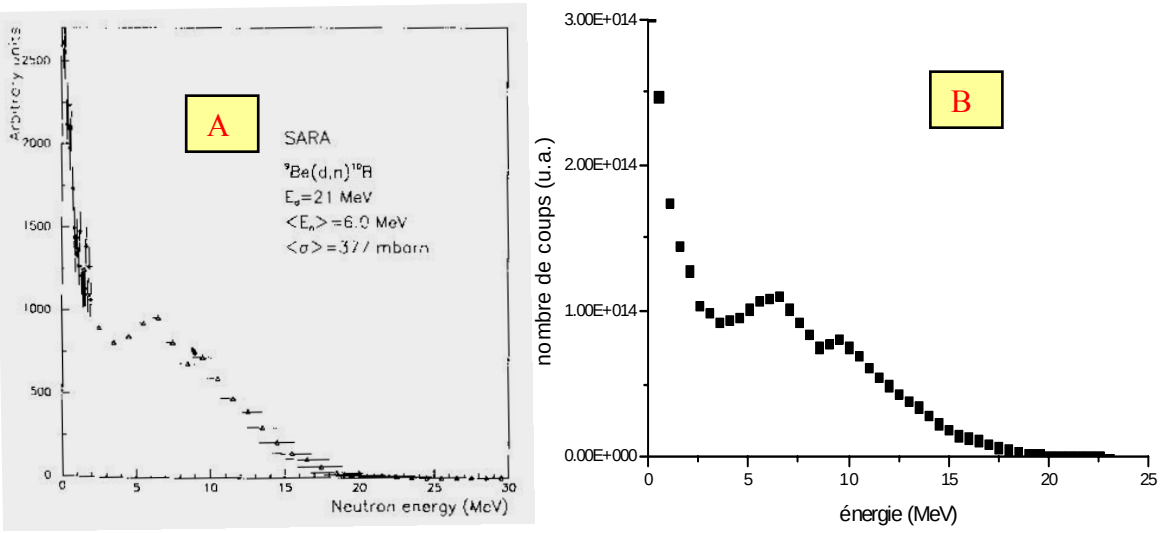

Figure 40: Measured (A) and computed (B) neutrons spectrum (SARA facility)

The computed neutrons spectrum (Fig. 40B) is in very good agreement with the experimental data (Fig. 40A) obtained previously with for SARA facility [22] at a maximum deuterons energy E_{max} =21MeV. Consequently, we can use with a high confidence the simulated neutrons spectrum in the case of the CERI facility (E_{max} =25 MeV).
Finally, the number of activated atoms N at the neutron energy ε is calculated using the well-known formulae:

$$N(\varepsilon) = \Phi(\varepsilon).\frac{m.N_A}{M}.\sigma(\varepsilon) \qquad (5)$$

Where Φ is the neutrons flux (neutrons/cm²), m the target thickness (g), N_A the Avogadro number, M the molar mass and σ(ε) the cross section of the reaction at the energy ε.
According to previous experiment, the integrated neutron dose expected at 8.5 cm from target with a deuteron beam of 21 MeV energy and 7μA current is in the range 0.9 -1.9.10^{15} n/cm² after an exposure time of 20 hours. Regarding the actual irradiation conditions (e.g., distance d=20cm, beam energy and current: 23 MeV and 35 μA, exposure time: 8 hours), the expected dose is in the range 0.32.10^{15}-0.7.10^{15} neutrons/cm².

Material activation

The cross sections are taken from the nuclear data base ENDF and calculations were focused only on the following reactions for the indium activation coming from the gasket of the test

cell: $^{115}In(n,\gamma)^{116}In$, $^{115}In(n,2n)^{114}In$, $^{115}In(n,p)^{115}Cd$, $^{115}In(n,\alpha)^{112}Ag$. Due to the short decay period and the rather low cross section and/or neutron flux in the energy range of interest, most of the above reactions don't produce high activation ten days after irradiation experiment. In contrast, $^{115}In(n,2n)^{114}In$ and $^{115}In(n,p)^{115}Cd$ reactions could induce enough activation: indeed the decay periods of the first excited states of ^{114}In and ^{115}Cd are respectively ~49 and ~45 days. In the worst case, if all produced nucleus are excited, it will induce respectively an activity above 600 kBq and 4 kBq ten days after irradiation. These results were confirmed by the actual tests: no significant activity has been detected from indium after irradiation experiment.

Neutron fluence measurements

Principle of nickel foils activation

The neutron fluences received by the actuators during irradiations are measured by means of an activation method of nickel foils, which are attached the tested actuators support using a Kapton film (Fig. 41).

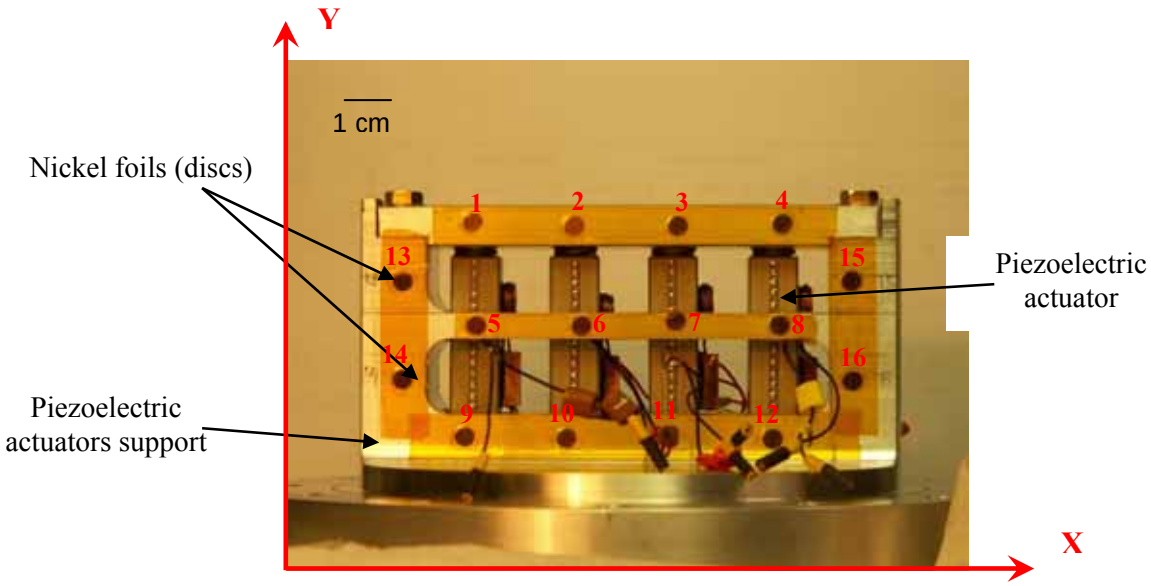

Figure 41: Locations of the nickel foils on the PICMA piezoelectric actuators support

The main characteristics of these nickel foils supplied by Goodfellow are summarized in Table 4.

Table 4: Values of the main characteristics of the nickel foils

Diameter (mm)	Thickness (mm)	Mass (mg)	Purity of Ni (%)
4	0.125	14.4	99.999

The activation method is based on the charge exchange reaction on ^{58}Ni :

$$^{58}Ni\ (n,p)\ ^{58}Co \qquad (6)$$

The determination of the nickel foils activity is performed by γ rays spectrometry. More precisely, we measure the gamma ray of ^{58}Co at 810 keV by means of a liquid nitrogen cooled ORTEC Ge-Li detector (T=77K). The main characteristics of this detector are illustrated in Table 5 and a photograph of the apparatus is shown in Fig. 42.

Table 5: Characteristics of the Ge-Li detector

Trademark	ORTEC
Type	8011-10185
Diameter of the crystal	43 mm
Length of the crystal	51.5 mm
Voltage	+ 4800 V
Resolution (FWHM) @ 1.33 MeV	1.77 keV
Relative efficiency	11.4%
Resolution @ 122 keV	1.08 eV

Figure 42: Gamma spectroscopy apparatus (detector and data acquisition system)

A close view photograph of the detector with lead shielding is presented in Fig. 43.

Figure 43: The detector with its Pb shielding

The resulting nickel activity A_{Ni} , deduced from g rays spectra such as that shown in Fig. 44, is then used for calculating the neutrons fluence Φ according to the formula:

$$\Phi = A_{Ni} / \sigma.N.\lambda \quad (7)$$

With:

N: number of atoms of ^{58}Ni per milligram of natural Ni

σ: mean activation cross section in cm²

λ: decay constant of ^{58}Co in seconde^{-1}

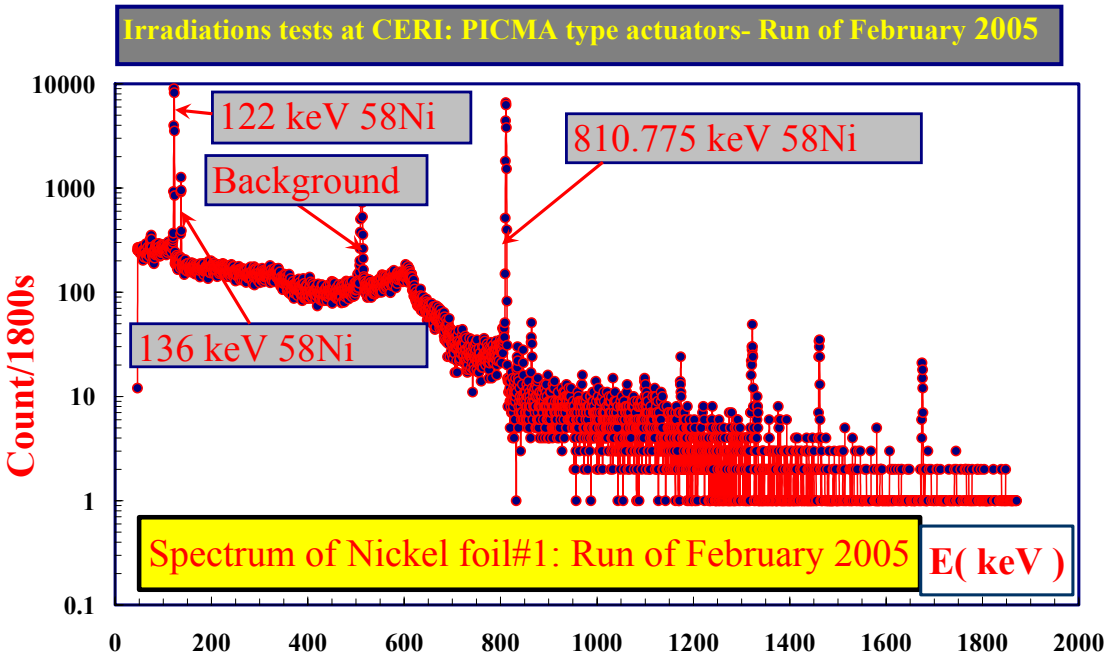

Figure 44: Typical spectrum of nickel foil #1 (Run of February 2005)

Note that for the calculations only ^{58}Ni radioisotope, which represents 68 % of natural nickel, is considered. Moreover, the lifetime of ^{58}Co is τ =70.864 days leading to decay constant λ (λ = Ln 2 / τ) of 1.13 x 10^{-7} seconde^{-1}.The values of the different parameters used in our calculations are given in Table 6.

Table 6: Values of the different parameters of the fluence calculations

N	σ (cm²)	λ (sec^{-1})
7 x 10^{18}	3.77 x 10^{-25}	1.13 x 10^{-7}

First experiment: PICMA piezoelectric actuators irradiations

The irradiation tests with fast neutrons of four PICMA actuators, at liquid helium temperature were performed during two days: 16th and the 17th of February 2005. For this test, the distance between the beryllium target and the piezoelectric actuators vertical mid plane is 25 cm. Each of the sixteen nickel foils was analyzed after 18 days and we obtained the neutron fluences map shown in Fig. 45.

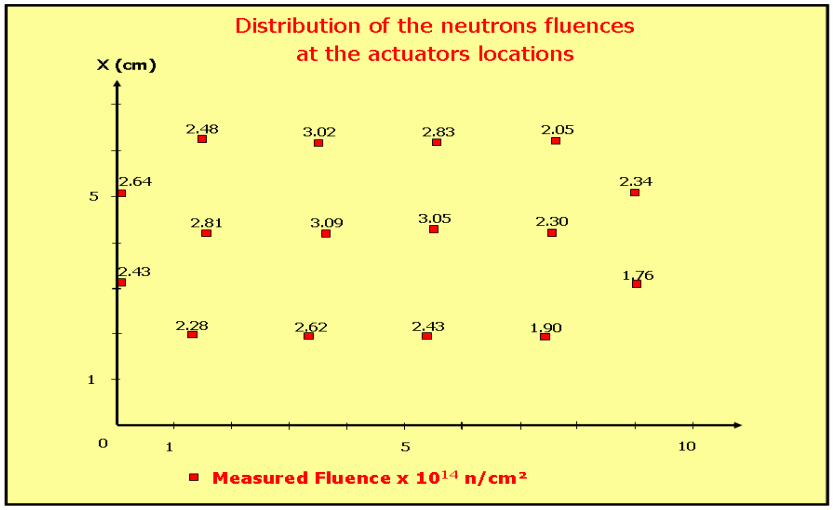

Figure 45: Neutrons fluence map for PICMA actuators irradiation

It might be stressed that during irradiation test the nickel foils # 13-14-15-16 were fallen, however the corresponding data are consistent with those of the other foils. The corresponding distribution is illustrated in Fig. 46. The histogram shows a relatively uniform fluence distribution: the mean value is 2.5 10^{14} n/cm^2 with a standard deviation of ±16%.

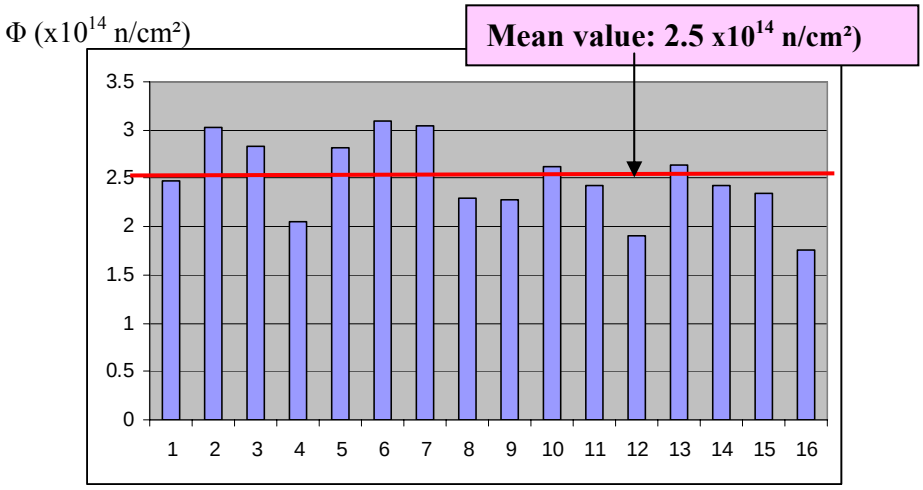

Figure 46: Neutrons fluence distribution for PICMA actuators irradiation

Second experiment: NOLIAC piezoelectric actuators irradiations

The second irradiation runs with fast neutrons of four NOLIAC actuators, at liquid helium temperature was performed during the 16th and the 17th of March 2005. In order to obtain higher neutron fluence, as compared to the previous test, the distance between the beryllium target and the piezoelectric actuators vertical mid plane was reduced from 25 cm to 20 cm. Moreover, we also measure the slow neutrons fluence with activation of Au foils (Fig. 47). The measured distribution is shown in Fig. 48.

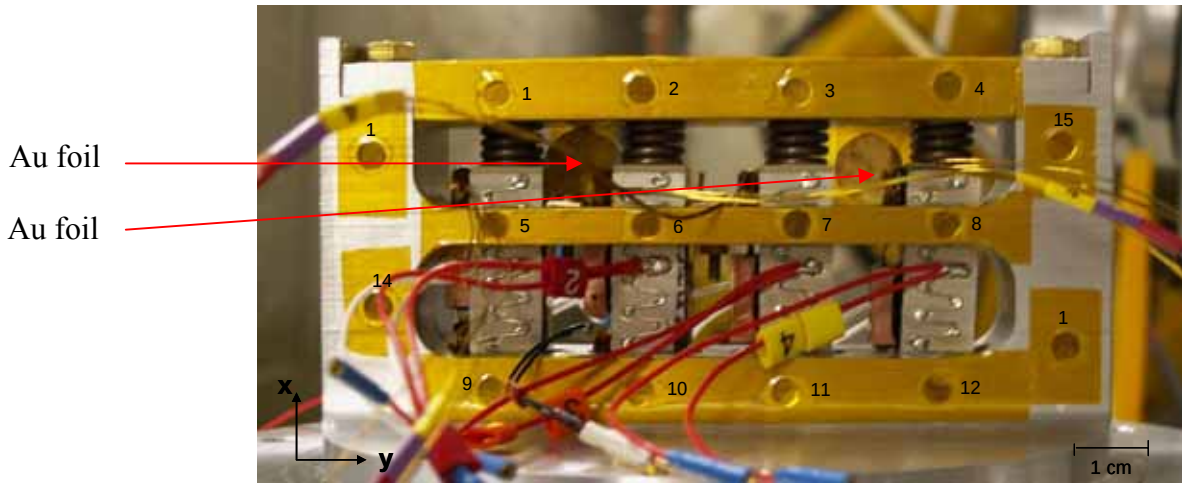

Figure 47: Distribution of the nickel foils on the NOLIAC piezoelectric actuators support

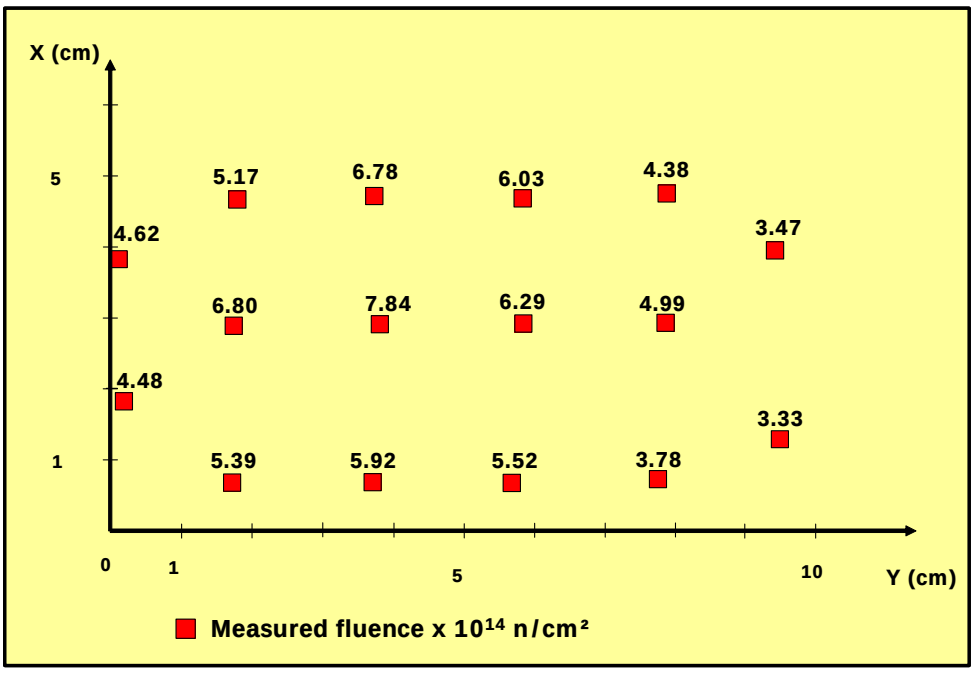

Figure 48: Neutron fluences distribution for NOLIAC actuators irradiation

Notice again that during irradiation tests, nickel foils # 13-14-16 were fallen (even with double layer of kapton film) but the corresponding fluences at their locations are consistent with the data in other regions. The resulting fluence distribution is illustrated in Fig. 49. This histogram shows a relatively uniform fluence distribution: the mean value is 5.3 10^{14} n/cm^2 with a standard deviation of ±24%. Our calculations for the slow neutrons fluence (e.g., energy range of 0.025 to 10^6 eV) give 2.42 10^7 n/cm²/s. Some neutron fluences measurements have also been performed on the cryostat at a distance of 35 cm from the target leading to mean value ~ 1.10^{14} n/cm².

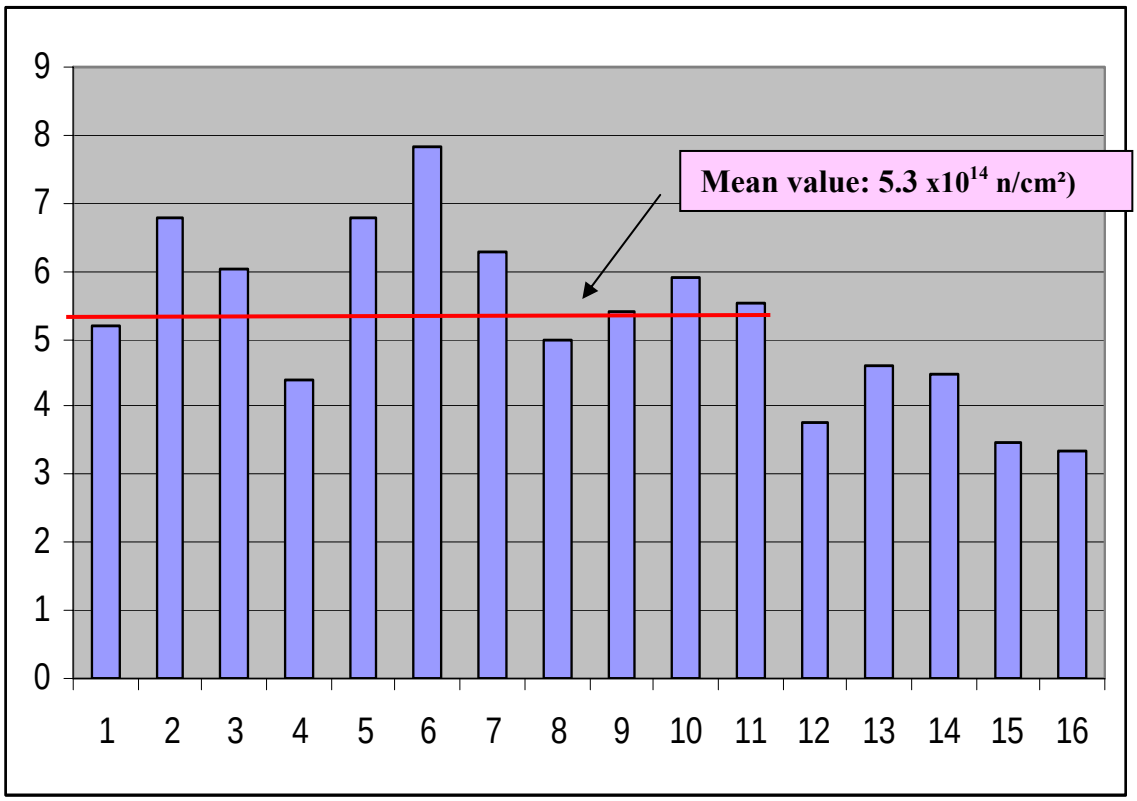

Figure 49: Neutrons fluence distribution for NOLIAC actuators irradiation

It should be emphasized that, by decreasing the distance between the target and the actuators by a factor 1.25, the neutron fluence increases by a factor of 2.1.

Third experiment: JENA piezoelectric actuators irradiations

The last irradiation campaign took place the 13th and the 14th of April 2005. The location of the nickel foils on the Piezosystem JENA piezoelectric actuators support is depisted in Fig.50. This photograph, which was taken after the irradiation, clearly show that nickel foils # 14-15-16 were fallen.

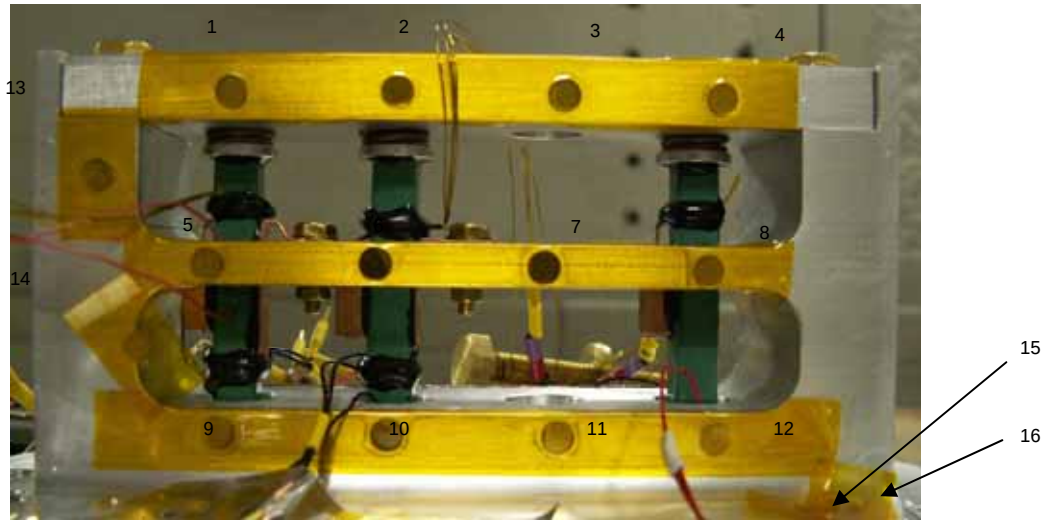

Figure 50: Distribution of the nickel foils on the JENA piezoelectric actuators support

Notice that for this irradiation run, the distance the beryllium target and the piezoelectric actuators is 20 cm. The analysis of the activity spectra of the 17 nickel foils leads to the neutron fluence map shown in Fig. 51.

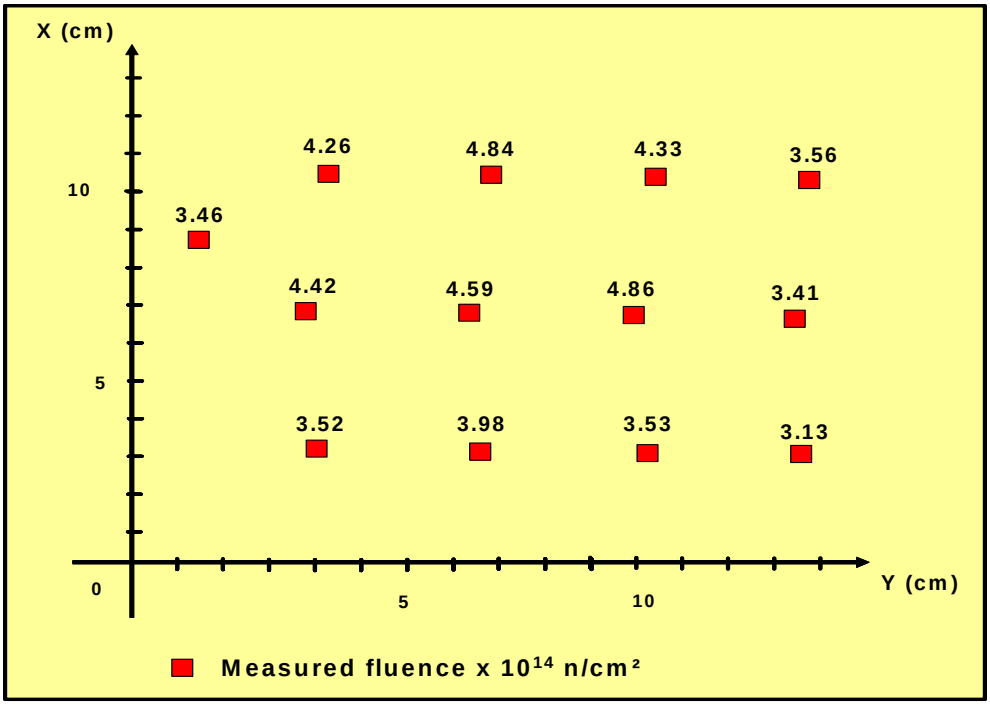

Figure 51: Neutron fluences distribution for JENA actuators irradiation

The corresponding distribution is illustrated by the histogram in Fig. 52. The mean value is 4.0 10^{14} n/cm^2 with a standard deviation of ±15%.

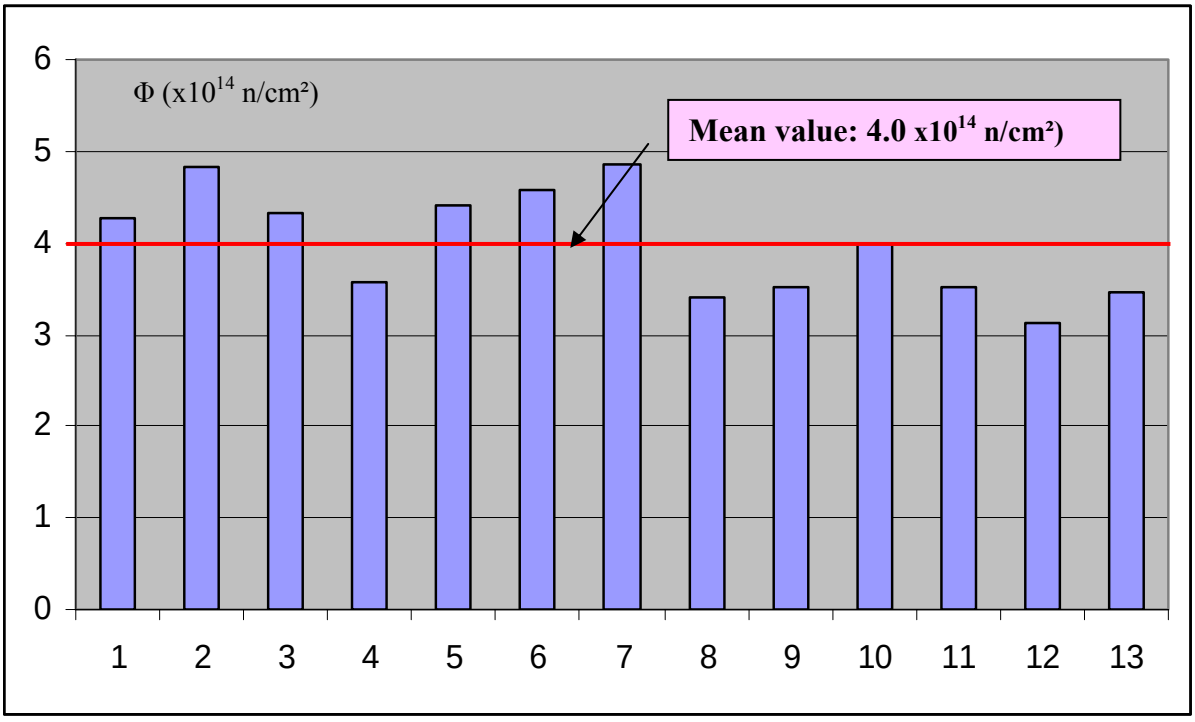

Figure 52: Neutrons fluence distribution for JENA actuators irradiation

We can notice that for Piezosystem JENA actuators, the neutron fluence is much lower than that observed for the test of NOLIAC actuators. This difference is mainly due to exposure durations, which are quite different: the durations of irradiation are 71880 s and 63900s for NOLIAC and Piezosystem JENA actuators respectively.

Effects of fast neutrons on electromechanical properties of actuators

After cool down to T=4.2K, the dielectric properties are measured without beam prior to radiation tests. Then, the actuators are subjected to fast neutrons radiation during ~20 hours and the dielectric properties, the temperatures of the piezostacks as well as beam parameters are on-line measured while the test-cell is maintained at 4.2K: the beryllium target is bombarded by the deuteron beam, the current of which is increased progressively from 1 µA to 35 µA. Finally, the dielectric properties measured after neutron exposure to a dose higher than 10^{14}neutrons/cm², are compared to the reference values before radiation. We briefly summarize the results, which are discussed in more details elsewhere [18]. As we have seen in a previous section, three beam tests were performed: four PICMA actuators in test #1, four NOLIAC actuators in test #2 and three Piezosystem JENA actuators for test #3. Notice that due to heating by neutrons beam, some parameters (e.g., C_p) increases with beam intensity. The experimental data for the three beam tests performed are illustrated in Fig. 53-Fig. 55.

Notice that for the data illustrated in Fig. 53-Fig. 54, the errors bars are calculated by considering the shift of Allen Bradley thermometers, which have been previously measured in a separate experiment [19-21].

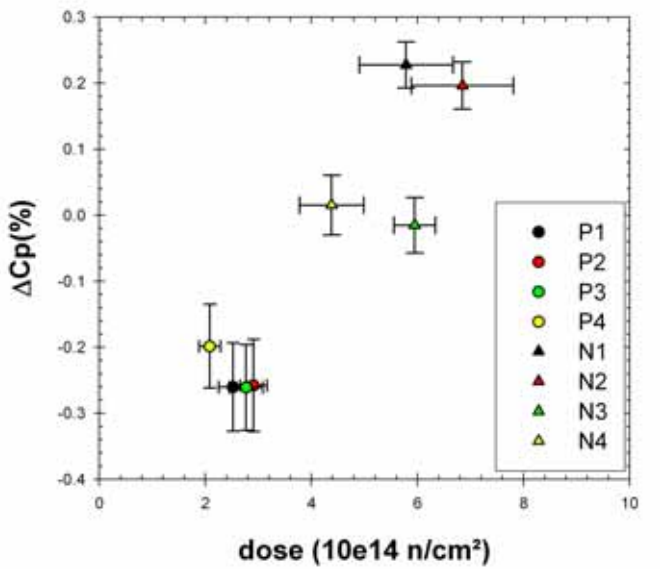

Figure 53: Effect of fast neutrons dose on capacitance at T=4.2 K.

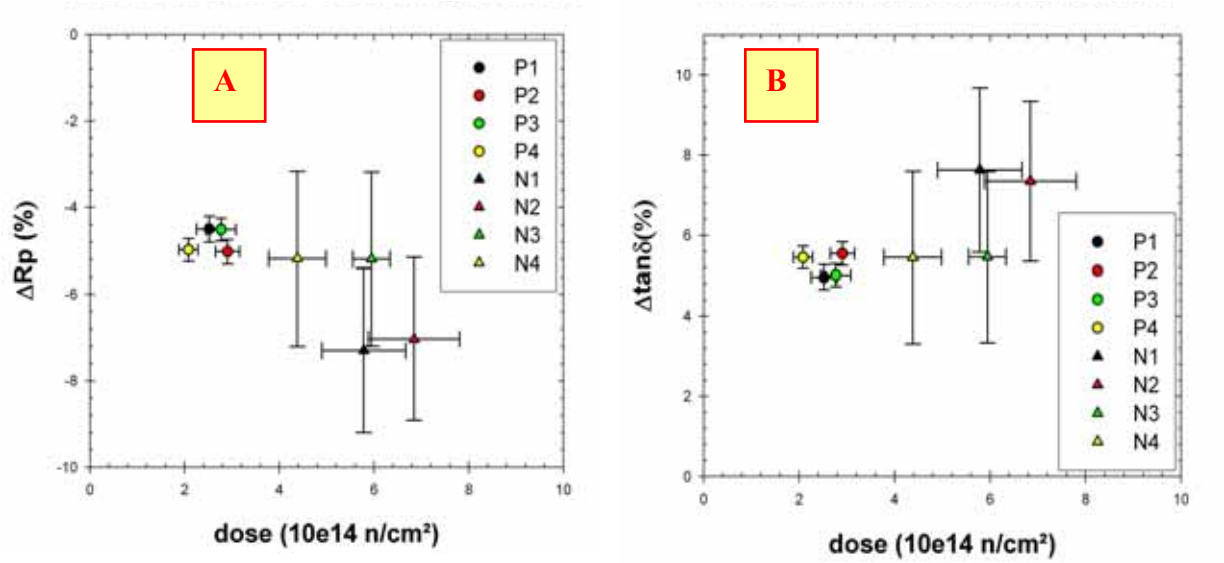

Figure 54: Effect of fast neutrons dose on parallel resistance (A) and loss factor (B).

In the range of neutrons dose investigated (2- 7.10^{14} n/cm^2), the data call for the following remarks: 1) the capacitance of the actuators of PICMA type Cp decreases by 0.25% when the fast neutrons dose is increased, b) the capacitance of the actuators of NOLIAC type Cp increases by 0.15% when the fast neutrons dose is increased, 3) for the two type of piezostacks the loss factor increases by 5 to 10 % when the fast neutrons dose is increased. In conclusion, no major damage was observed but slight performance degradation may be due to aging effect, is measured: these piezostacks are suited for use in cryogenic and neutrons radiation environment up to a total dose ~ 7.10^{14} n/cm^2.

Integration of the piezostacks into the Saclay piezo-tuner

In the frame of CARE WP8, IPN Orsay had prepared two piezoelectric actuators PICMA 6 and PICMA 7 (Fig. 55) for their integration [25] in the new PiezoTuning System (PTS) developed at Saclay [26]. The fixture of the actuators is a critical part of the PTS so it was carefully designed to fulfil two main requirements: 1) avoid shear forces and/or torsion forces to the actuator, 2) fit very precisely (e.g. ~10 µm tolerance in the longitudinal direction or axis of the piezostacks) into the PTS in order to avoid loss of mechanical contact during cool down to 2 K. To fulfil the first requirement, a cone on sphere system is used: a) two hemispherical stainless steel pieces are glued at each extremity of the piezostacks (Bonding agent: epoxy STYCAST 2850FT), b) two stainless steel holders conically shaped are sandwiched between the actuator and the fixture. Note that a mechanical preloading to the actuator is needed in order to increase the life time for dynamic operation (i.e. pulsed mode of the accelerator). In the actual PTS, the cavity acting as a spring is used for preloading the piezostacks.

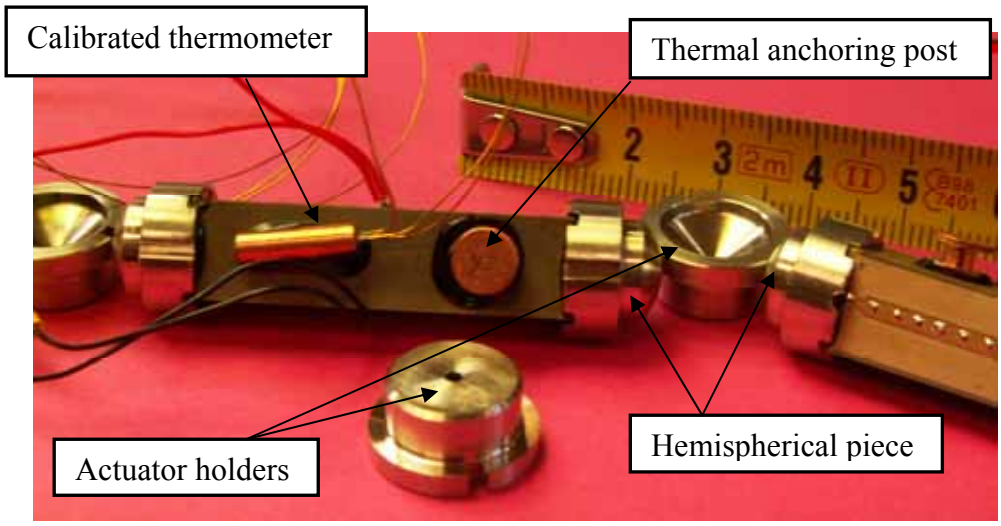

Figure 55 : Piezoelectric actuators ready for integration into Saclay PTS

The overall lengths L of the actuators, including their holders (Fig. 56), were measured with a high precision by the company Gavard who fabricated these elements leading to the following values: L_6=51mm $_{-0}^{+5\mu m}$ and L_7=51mm $_{-0}^{+7\mu m}$ for the piezostacks PICMA6 and PICMA7 respectively.

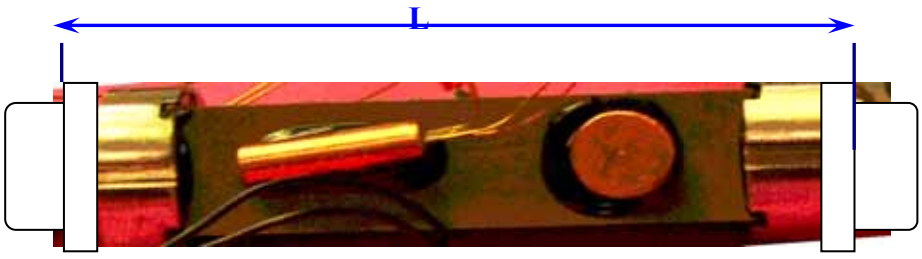

Figure 56: Definition of the overall length L

Further, precise measurements were performed by Gavard company using micrometer and three-dimensional machine: the data are within the specifications illustrated in Table 6.

Table 6: Comparison of the measured dimensions with the specifications

Specification	Measured
$15^{+0.2}$	15.11
7.5	7.5
Φ12g6	11.987
3.01	3.01
Φ11	11.02
4.7	4.69
60°	60°
1.7	1.72
$6.25^{-0.2}$	6.1
Φ1.5	1.52

Moreover, each actuator is equipped with an Allen-Bradley thermometer (Table7), which was calibrated at IPN Orsay facility [27] (Fig. 57) in the temperature range 1.56 K-71 K.

Table7: References of the calibrated thermometers

Piezoelectric actuator	Thermometer
PICMA#6	CRT_AB_5038N17
PICMA#7	CRT_AB_5038N18

Table7: References of the calibrated thermometers

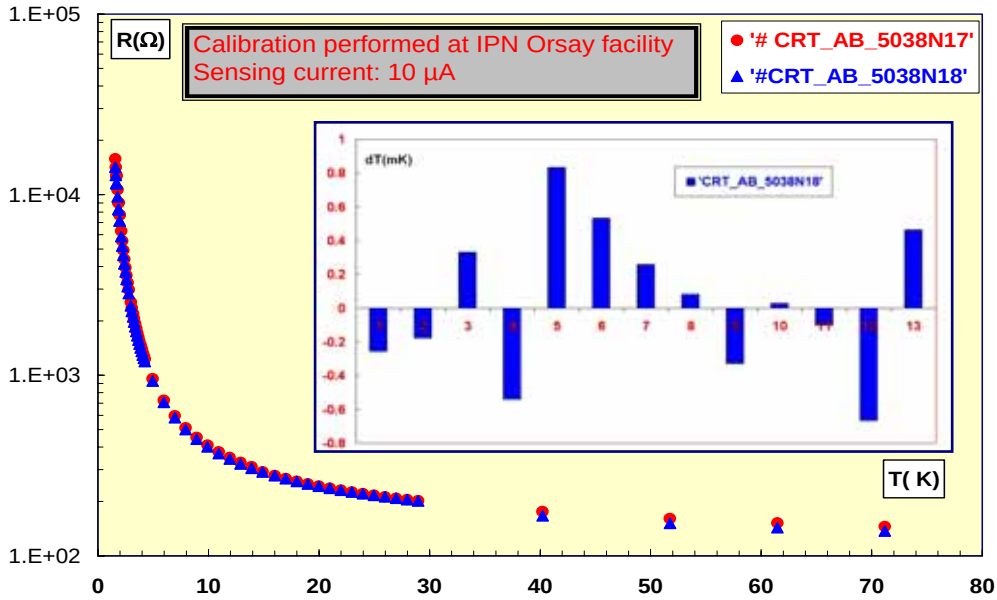

Figure 57: Calibration curves and fit error histogram (insert) in superfluid helium region (1.56 K-2.1 K).

We performed the measurements of the electrical properties of the piezostacks before and after their integration into the PTS. These tests were done with a LCR meter at room temperature (T~300 K) and the results are shown in Table 8 (actuators free) and Table 9 (actuators in PTS). The observed differences (i.e., Cp, Rp and tg(δ)) are due to preloading.

Table 8: Electrical properties of actuators before integration in PTS (T~300K, sensing voltage: amplitude =1 V amplitude, frequency =100Hz, four wires method)

Piezostacks	PICMA#6	PICMA#7
Capacitance (µF)	12.63	12.92
Parallel resistance (kΩ)	5.07	3.53
Loss tangent	1.2410^{-2}	1.2710^{-2}
Impedance module (Ω)	126.0	123.0
Impedance phase (°)	-87.56	-88.55

Table 9: Electrical properties of actuators after integration in PTS (T~300K, sensing voltage: 1 V amplitude, frequency : 100Hz, two wires)

Piezostacks	PICMA#6	PICMA#7
Capacitance: Cp (µF)	12.58	12.87
Parallel resistance: Rp (kΩ)	3.41	3.53
Loss tangent: tg(δ)	1.8510^{-2}	1.9510^{-2}
Impedance module (Ω)	126.4	123.6
Impedance phase (°)	-87.88	-88.10

Installation on the cavity in CRYHOLAB

The actuators were integrated into the PTS then the assembly was mounted on the cavity C45 and installed in CRYHOLAB test facility (Fig. 58). The whole device is now ready for cryogenic tests which started on April 11, 2006.

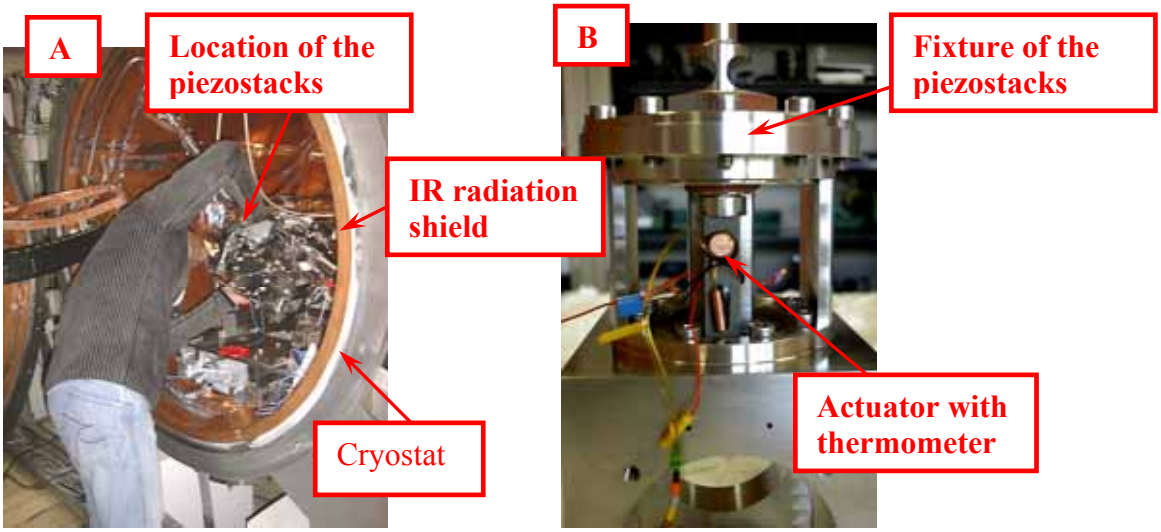

Figure 58: A) Mounting the PTS in CRYHOLAB, B) close view to the fixture of actuators for integration in the tuner.

Typical values of the piezostacks properties measured at the cavity operating temperature T=2K are listed in Table 10.

Table 10: Typical values of electromechanical properties of piezostacks measured at T=2 K

Parameter: name (unit)	PICMA	NOLIAC
Capacitance: Cp (µF)	2.74	1.46
Parallel resistance: Rp (kΩ)	105	132
Impedance module (Ω)	581	1090
Impedance phase (°)	-89.7	-89.5
Loss tangent: tg(δ)	$2.85\ 10^{-3}$	$4.15\ 10^{-3}$
Rp.Cp (ms)	286	193
Displacement: ΔX(µm) @Vmax	3 @120V	3@150V

Description of the experiments

In order to investigate the electro-acoustic behaviour of the TESLA type cavity #C45 and measure the performance of the PTS developed at Saclay with PICMA actuators, the following tests in CRYHOLAB are planned for three weeks (10-27 April 2006):

1) Measurements of the transfer functions,
2) Study of the mechanical modes of the cavity including quality factors,
3) Study Lorentz detuning and detuning compensation with PTS,
4) Measurements of the actuators response to the applied preloading force.

The block diagram of the transfer function experiment is shown in Fig. 59. The test consists of measuring the amplitude and phase of the transmitted RF signal (through the mixer) as function of the frequency of the mechanical vibration of the structure generated by the piezoelectric actuator. The measurements were already performed at Room Temperature (R.T) on the cavity #C45with its Lhe tank. The first experimental data were published elsewhere [28] and will be thoroughly presented and discussed in a separate report as a part of WP10 activity dedicated to integrated RF tests in a horizontal cryostat.

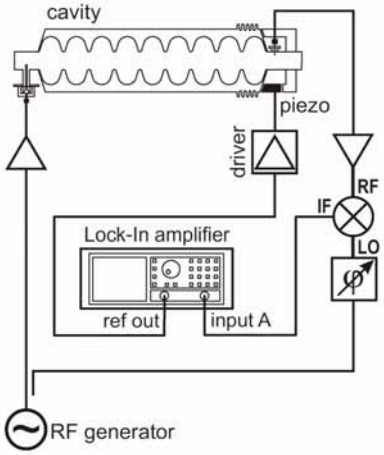

Fig. 59: Block diagram of the experimental set-up

Publications

A large part of the present work was published and/or presented at different international conferences as illustrated in Table 11. A total of fifteen publications were produced: a) one journal paper, b) eleven in conferences proceedings including three talks, c) three CARE notes. More journal papers are in preparation and will be published in few months.

Table 11. List of publications for IN2P3 tuner activities

Paper#	Title	Authors	Journal/Conf.
1	**"Measurement of static force in liquid helium temperature"**	P. Sekalski, A. Napieralski, DMCS, Technical University of Lodz, Poland, M. Fouaidy, IPNO, Universté Paris-Sud 11, CNRS/IN2P3, France, A. Bosotti, R. Paparella, INFN Milan, Italy	Measurement science and technology
2	**"Characterization of piezoelectric actuators used for SRF cavities active tuning at low temperature"**	M. Fouaidy, N. Hammoudi, IPNO, Universté Paris-Sud 11, CNRS/IN2P3, France	SRF 2003
3	**"Static Absolute Force Measurement for Preload Piezoelements Used for Active Lorentz Force Detuning System",**	S. P. Sekalski, A. Napieralski, TUL, Lodz, Technical University of Lodz**,** A. Bosotti INFN/LASA, M. Fouaidy, IPNO, Universté Paris-Sud 11, CNRS/IN2P3, France, L. Lilje, S. Simrock DESY, R. Paparella, P.F. Puricelli, INFN Milano, Italy	LINAC 2004
4	**"Full Characterization at Low Temperature of Piezoelectric Actuators Used for SRF Cavities Active Tuning"**	M. Fouaidy, G. Martinet, N.Hammoudi, F.Chatelet , S.Blivet, A. Olivier, H. Saugnac, IPNO, Universté Paris-Sud 11, CNRS/IN2P3, France	PAC05
5	**"Static and dynamic properties of piezoelectric actuators at low temperature and integration in SRF cavities cold tuning system"**	M. Fouaidy, G. Martinet, N. Hammoudi, F. Chatelet, N. Gandolfo , H. Saugnac, S. Bousson IPNO, Universté Paris-Sud 11, CNRS/IN2P3, France	MIXDES2005
6	**"Electromechanical, thermal properties and radiation hardness tests of Piezoelectric Actuators at Low Temperature"**	M. Fouaidy, G. Martinet, N. Hammoudi, F. Chatelet, A. Olivier, S. Blivet, H. Saugnac, A. Le Goff, IPNO, Universté Paris-Sud 11, CNRS/IN2P3, France	SRF 2005
7	**"Cold tuning system for 700 MHz elliptical superconducting Cavity for protons accelerator"**	M. Fouaidy, N. Hammoudi, N. Gandolfo, S. Rousselot, M. Nicolas, P. Szott, S. Blivet, H. Saugnac, S. Bousson, IPNO, Universté	SRF2005

		Paris-Sud 11, CNRS/IN2P3, France	
8	**"Smart materials based system operated at 2K used at superconducting cavity tuner for VUV-FEL purpose"**	P. Sekalski, A. Napieralski, DMCS, Technical University of Lodz, Poland, S. Simrock, C. Albrecht, L. Lilje, Desy, Hamburg, Germany P. Bosland, M. Fouaidy, N. Hammoudi, IPNO, Universté Paris-Sud 11, CNRS/IN2P3, France A. Bosotti, R. Paparella, INFN Milano, Italy	ACTUAORS2006
9	**"Low temperature properties of piezoelectric actuators used in SRF cavities cold tuning systems"**	G. Martinet, M. Fouaidy, N. Hammoudi, A. Olivier, F. Chatelet, S. Blivet, H. Saugnac, IPNO, Universté Paris-Sud 11, CNRS/IN2P3, France	EPAC2006
10	**"Electromechanical characterization of piezoelectric actuators subjected to a variable preloading force at cryogenic temperature"**	M. Fouaidy, M. Saki, N. Hammoudi, L. Simonet, IPNO, Universté Paris-Sud 11, CNRS/IN2P3, France	EPAC2006
11	**"Low temperature electromechanical and dynamic properties of piezostacks for superconducting RF cavities fast tuners"**	Fouaidy M., Martinet G., Hammoudi N., IPNOrsay, France IPNO, Universté Paris-Sud 11, CNRS/IN2P3, France	CRYOPRAGUE2006
12	**"Active compensation of Lorentz force detuning of a TTF 9-cell cavity in CRYHOLAB"**	G. Devanz, P. Bosland, M. Desmons , E. Jacques, M. Luong, B. Visentin, CEA-Saclay, France M. Fouaidy, IPNO, Universté Paris-Sud 11, CNRS/IN2P3, France	LINAC2006
CARE-Note-2006-006-SRF	"**Integration of piezoelectric actuators in the piezotuner developed at Saclay"**	M. Fouaidy, N. Hammoudi, G. Martinet, IPNO, Universté Paris-Sud 11, CNRS/IN2P3, France G. Devanz, P. Bosland, E. Jacques, Sylvie Regnaud, CEA Saclay, France	
CARE-Note-2006-007-SRF	**"Electromechanical characterization of piezoelectric actuators subjected to a variable preloading force at cryogenic temperature"**	M. Fouaidy, M. Saki, N. Hammoudi, L. Simonet, IPNO, Universté Paris-Sud 11, CNRS/IN2P3, France	
CARE-Note-2006-007-SRF	**"Radiation hardness tests of piezoelectric actuators with fast neutrons at liquid helium temperature"**	M. Fouaidy, G. Martinet, N. Hammoudi, F. Chatelet, A. Olivier, S. Blivet, F. Galet, IPNO, Universté Paris-Sud 11, CNRS/IN2P3, France	

Status of activities

All the tasks of IN2P3 tuner activities are completed as listed in Table 12.

Table 12. Status of IN2P3 tuner activities

Nr.	Task	Status March 07
8.4	IN2P3 Activity	100%
8.4.1	Characterize actuators/piezo-sensors at low temperature	100%
8.4.2	Report on actuator/piezo sensor	100%
8.4.3	Test radiation hardness of piezo tuners	100%
8.4.4	Report on radiation hardness tests	100%
8.4.5	Integration of piezo and cold tuner	100%
8.4.6	Cryostat tests	100%
8.4.7	Tests with pulsed RF	100%
8.4.8	Report on IN2P3 tuner activities	100%

Conclusion

Three dedicated apparatus were developed for the full characterization of piezoelectric actuators at low temperature. Several industrial low voltage multilayer piezostacks, based on PZT material and supplied by three different companies were successfully tested: their electromechanical, dynamic and thermal propertied were measured at cryogenic temperatures in the range 1.8 K- 300 K. For the piezostacks Piezosystem JENA type, the measured parameters show large variations from a series production to another. Moreover, the full range displacement of theses actuator decreases strongly with temperature from ~42 µm at room temperature down to 2.3 µm at 1.8K. Notice that for T ≤ 10 K, this full range displacement stay nearly constant. The dielectric losses for a sinusoidal displacement of 1 µm amplitude at 1.8 K at a frequency of 100 Hz are lower than 1mW. These actuators are not suited for Lorentz detuning compensation in superconducting RF cavities, because they don't full fill the needed requirements: 1) maximum stroke less than 2 µm at 2K while 3 µm are required, 2) their blocking force ~1kN at 300 K is much lower than the required 3 kN, 3) their mechanical stiffness ~25N/µm is four time lower than needed. (e.g., 100N/µm). Finally, due to a lack of fabrication reproducibility from batch to batch (i.e., different behaviour of ΔX vs. T) and their very short lifetime when operated at 2 K (e.g., electrical breakdown and/or mechanical damages), such actuator could not be used in future accelerators (e.g., XFEL, ILC) where a large number of these components is needed and the demanding reliability and availability of the machine. For the actuators of PICMA and NOLIAC type, the full range displacement decreases also strongly with temperature from ~40µm at room temperature down to 2.8µm-3µm at T=1.8K leading to a theoretical detuning compensation Δf≈1kHz close to the requirement for TESLA nine cells cavities operating at an accelerating gradient for 33 MV/m. Moreover, as for these two types of piezostacks neither electrical breakdown nor damage observed during the tests at cryogenic temperatures, the lifetime is not an issue.

For all type of piezostacks tested including Piezosystem JENA actuators, the experimental data show that at low temperature (e.g., T<80 K), the capacitance is proportional to the full range displacement. Consequently, it constitutes a simple mean for indirect and automatic calibration of a large number of actuators: capacitance measurements are easier and much time consuming as compared to the true calibration (e.g., displacement versus voltage characteristics at different temperatures). As previous studies showed that the life time of piezostacks depends strongly on the applied preloading force, we developed a second apparatus for investigating the effect of preloading on the electromechanical and dynamic properties of actuators at cryogenic temperatures. At a given temperature, the capacitance of the piezostacks increases linearly with the applied axial preloading force up to 4 kN: this linear dependence is observed in the whole temperature rage 2.8 K-300 K and with a very good reproducibility. Moreover, the sensitivity of the piezostacks to preloading decreases strongly with temperature from 426nF/kN at T=300K to 16nF/kN at T=2 K. Furthermore, we studied the behaviour of the piezostacks as dynamic force sensor when subjected to step force variation. The data show the reversibility and the linearity of the response with high repeatability: 1) the peak voltage is proportional to preload variation ΔF and change de sign with ΔF, 2) the actuator exhibit a good sensitivity with a peak voltage ~6.5 V/kN at T=4.2K. This property will be used for in situ precise measurement of the force applied to the actuators integrated in the tuning system and mounted on the cavity in operation. Furthermore, a third facility was developed for studying the effect of fast neutrons on the electromechanical properties of piezoelectric actuators at liquid helium temperature (T=4.2K). Three beam tests were then performed: four actuators of PICMA type, four actuators of NOLIAC and three actuators from Piezosystem JENA were subjected to irradiation tests at T=4.2 K with a fast neutrons beam (Energy spectrum: 1-20MeV). A total averaged dose ranging from 2.510^{14}n/cm^2 to 5.310^{14}n/cm^2 was achieved in ~20hours. In the range of neutrons dose investigated, the data following main conclusions could be drawn: 1) the capacitance of the actuators of PICMA type Cp decreases by 0.25% when the fast neutrons dose is increased, b) the capacitance of the actuators of NOLIAC type Cp increases by 0.15% when the fast neutrons dose is increased, 3) for the two type of piezostacks the loss factor increases by 5 to 10 % when the fast neutrons dose is increased. Thus, neither damage nor anomalous behavior was observed but slight performance degradation may be due to aging effect, is measured: these piezostacks are suited for use in cryogenic and neutrons radiation environment up to a total dose ~ 7.10^{14} n/cm^2. Finally, two actuators of PICMA type were prepared and integrated into the new cold tuning system developed at Saclay. This new fast active cold tuning system was mounted on a TESLA cavity and successfully tested at high RF power in the horizontal cryostat facilities CRYHOLAB at Saclay with the expected performance. This cold tuning system will help greatly for the optimum operation of superconducting RF cavities operating at high gradient in pulsed mode. It will allow the efficient transfer of the RF power from the source to the particle beam to be accelerated and to damp the micro-phonics resulting in a better beam quality in term of energy dispersion.

ACKNOWLEDGEMENT

We acknowledge the support of the European Community-Research Infrastructure Activity under the FP6 “Structuring the European Research Area” program (CARE, contract number RII3-CT-2003-506395)

References

1 D. Edwards, 'Conceptual Design Report for the TESLA Test Facility', DESY Print, 1995.
2 J. Andruszkow et al., "TESLA The Superconducting Electron-Positron Linear Collider with an Integrated X-Ray Laser Laboratory- Technical Design Report, Part II : The Accelerator", Editors R.Brinkmann, K. Flöttmann, J.Rossbach, P. Schmüser, N. Walker, H. Weise, March 2001.
3 R. Brinkmann et al., 'TESLA XFEL, Technical Design Report Supplement', DESY 2002-167, 2002.
4 A. Gamp, 'On the preference of cold RF technology for the international linear collider', TESLA Report 2005-23, 2005.
5 M. Liepe et al., ''Dynamic Lorentz Force Compensation with a Fast Piezoelectric Tuner'', PAC 2001,Chicago,USA, June 2001, p.1074.
6 A. Leuschner, S. Simrock, "Radiation field inside the tunnel of the linear collider TESLA", Laboratory Note, DESY D3-113, 2000.
7 M. Fouaidy, N. Hammoudi, IPN Orsay, "Characterization of piezoelectric actuators used for SRF cavities active tuning at low temperature", Proceedings of the 11th Superconducting Radio Frequency workshop (SRF 2003), Sept. 2003, Travemunde, Germany,
8 K. G. Vandervoort et al., Rev. Sci. Instrum., Vol. 64, (1993), p. 896-899.
9 M. Locatelli et al., Rev. Sci. Instrum., Vol. 59, (1988), p. 661.
10 M. Fouaidy, G. Martinet, N.Hammoudi, F.Chatelet , S.Blivet, A. Olivier, H. Saugnac "Full Characterization at Low Temperature of Piezoelectric Actuators Used for SRF Cavities Active Tuning", Proc. PAC05, Knoxville, Tennessee (USA), May 2005.
11 M. Fouaidy, G. Martinet, N. Hammoudi, F. Chatelet, A. Olivier, S. Blivet, H. Saugnac, A. Le Goff, "Electromechanical, thermal properties and radiation harness tests of Piezoelectric Actuators at Low Temperature", Proc. SRF2005, Ithaca, New York (USA), July 2005.
12 G. Martinet, M. Fouaidy, N.Hammoudi, A. Olivier, F.Chatelet , S.Blivet, H. Saugnac, "Low temperature properties of piezoelectric actuators used in SRF cavities cold tuning systems", to be presented at EPAC06, Edinburgh, (Scotland), 26-30 June 2006.
13 Fouaidy M., Martinet G., Hammoudi N., "Low temperature electromechanical and dynamic properties of piezostacks for superconducting RF cavities fast tuners", CRYOPRAGUE 200-, Praha, Czek republic, July 2006.
14 R. Bindig, G. Helke, "Application of piezoceramic multilayer actuators, experiences and solution ", Actuator 2000, Bremen, Germany.
15 M. Fouaidy, M. Saki, N. Hammoudi, L. Simonet, "Electromechanical characterization of piezoelectric actuators subjected to a variable preloading force at cryogenic temperature", CARE-Note- 2005- 007- SRF.
16 M. Fouaidy, M. Saki, N. Hammoudi, L. Simonet, "Electromechanical characterization of piezoelectric actuators subjected to a variable preloading force at cryogenic temperature", to be presented at EPAC06, Edinburgh, (Scotland), 26-30 June 2006.
17 M. Saki, "Electromechanical characterization of piezoelectric actuators subjected to a variable preloading force at cryogenic temperature", M. Sc Thesis, text in french, Université de Versailles Saint Quentin en Yvelines, July 2005.
18 M. Fouaidy, G. Martinet, N. Hammoudi, F. Chatelet, A. Olivier, S. Blivet, F. Galet, "Radiation hardness tests of piezoelectric actuators with fast neutrons at liquid helium temperature", CARE-Note-07-004-SRF.
19 T. Junquera et al., 'Neutrons irradiation tests of calibrated cryogenic sensors at low temperature', Proc. CEC-ICMC' 97, 29 July- 1 August 1997, Portland, USA.

20 J.F Amand et al., 'Neutron irradiation tests of pressure transducer in liquid helium', Proc. CEC-ICMC, 12-16 July 1999, Montreal, Canada
21 J.F Amand et al., 'Neutron irradiation tests in superfluid helium of LHC cryogenic thermometers', Proc. ICEC17, 14-17 July 1998, Bournemouth, UK
22 J. Collot et al., NIM A 350 (1994), p. 525.
23 J. C Parnell Br. J. Radiol., 45 (1972) 542.
24 L. Maunoury, "Production de faisceaux d'ions radioactifs multi-chargés pour SPIRAL: études et r2alisation du premier ensemble cible-source", PhD Thesis, Université de CAEN, GANIL T 98-01, 1998.
25 M. Fouaidy, N. Hammoudi, G. Martinet, IPNO, Universté Paris-Sud 11, CNRS/IN2P3, France, G. Devanz, P. Bosland, E. Jacques, Sylvie Regnaud, CEA Saclay, France, "Integration of piezoelectric actuators in the piezotuner developed at Saclay", CARE-Note-2006-006-SRF.
26 P. Bosland, Bo Wu, "Mechanical study of the 'Saclay piezo tuner' PTS (Piezo Tuning System", CARE-Note- 2005- 004- SRF.
27 E. Chanzy, T. Junquera, J. P. Thermeau, S. Buhler, C. Joly, J. Casas-Cubillos, C. Balle, "Cryogenic thermometer calibration system using a helium cooling loop and a temperature controller", Proc. ICEC17, Bournemouth (UK), July 1998.
28 G. Devanz, P. Bosland, M. Desmons , E. Jacques, M. Luong, B. Visentin, CEA-Saclay, France, M. Fouaidy, IPNO, Universté Paris-Sud 11, CNRS/IN2P3, France, "Active compensation of Lorentz force detuning of a TTF 9-cell cavity in CRYHOLAB", Proc. LINAC 2006, August 21-25, Knoxville, TN, USA.